Impact of solar EUV flux on CO Cameron band and CO_2^+ UV doublet emissions in the dayglow of Mars

Sonal Kumar Jain*and Anil Bhardwaj†
Space Physics Laboratory,
Vikram Sarabhai Space Centre,
Trivandrum, India - 695022

Planetary and Space Science, 2011, doi:10.1016/j.pss.2011.08.010

Abstract

This study is aimed at making a calculation about the impact of the two most commonly used solar EUV flux models – SOLAR2000 (S2K) of Tobiska (2004) and EUVAC model of Richards et al. (1994) – on photoelectron fluxes, volume emission rates, ion densities and CO Cameron and CO_2^+ UV doublet band dayglow emissions on Mars in three solar activity conditions: minimum, moderate, and maximum. Calculated limb intensities profiles are compared with SPICAM/Mars Express and Mariner observations. Analytical yield spectrum (AYS) approach has been used to calculate photoelectron fluxes in Martian upper atmosphere. Densities of prominent ions and CO molecule in excited triplet $a^3\Pi$ state are calculated using major ion-neutral reactions. Volume emission rates of CO Cameron and CO_2^+ UV doublet bands have been calculated for different observations (Viking condition, Mariner and Mars Express SPICAM observations) on Mars. For the low solar activity condition, dayglow intensities calculated using the S2K model are ∼40% higher than those calculated using the EUVAC model. During high solar activity, due to the higher EUV fluxes at wavelengths below 250 Å in the EUVAC model, intensities calculated using EUVAC model are slightly higher (∼20%) than those calculated using S2K model. Irrespective of the solar activity condition, production of Cameron band due to photodissociative excitation of CO_2 is around 50% higher when S2K model is used. Altitude of peak limb brightness of CO Cameron and CO_2^+ UV doublet band is found to be independent of solar EUV flux models. Calculated limb intensities of CO Cameron and CO_2^+ UV doublet bands are on an average a factor of ∼2 and ∼1.5, respectively, higher than the SPICAM Mars Express observation, while they are consistent with the Mariner observations.

1 Introduction

First observation of CO Cameron and CO_2^+ UV doublet emissions in the Martian dayglow were made by the Mariner 6 and 7 flybys in 1969–1970 (Barth et al., 1971; Stewart, 1972). These observations provided an opportunity to study the Martian upper atmosphere in a greater detail. The CO Cameron band ($a^3\Pi - X^1\Sigma^+$; 180 – 260 nm) system arises due to the transition from the excited triplet $a^3\Pi$ state, which is the lowest of triplet states, to the ground state $X^1\Sigma^+$ of CO. Doublet transition ($B^2\Sigma^+ - X^2\Pi$) from excited CO_2^+ ($B^2\Sigma_u$) to the ground state CO_2^+ ($X^2\Pi$) gives emission in ultraviolet wavelengths at 288.3 and 288.6 nm. Apart from these emissions, Fox-Duffenback-Berger band of CO_2^+ ($A^2\Pi_u$ – $X^2\Pi_g$), fourth positive band of CO, first negative band of CO^+ (B – X), and several atomic line emissions of carbon and oxygen atoms were also recorded by Mariner 6, 7, and 9 (Barth et al., 1971; Stewart, 1972; Stewart et al., 1972). With the help of theoretical calculations and laboratory measurements, Barth et al. (1971) proposed possible mechanisms for the dayglow emission observed in the Martian atmosphere. Maximum intensity of CO Cameron band and

*sonaljain.spl@gmail.com
†anil_bhardwaj@vssc.gov.in; bhardwaj_spl@yahoo.com

UV doublet observed by Mariner 6 and 7 were 600 kR at ∼131 km and 35 kR at 148 km, respectively.

Emissions from Cameron band and CO_2^+ UV doublet bands were also observed in 1971–1972 by Mariner 9, the first spacecraft to orbit Mars. Stewart et al. (1972) observed a reduction in the intensity of Cameron band by a factor of 2.5 compared to Mariner 6 and 7 observations. They attributed this difference to the reduction in the solar activity and better calibration of Mariner 9 instrument. The observed maximum slant intensities of CO Cameron band were between 200 and 300 kR and averaged topside scale height for the same band was 17.5 km. Stewart (1972) also observed a good correlation between CO Cameron band intensity and solar F10.7 flux, which suggest that these emissions are controlled by the incident solar photon flux.

Since the Mariner 6, 7, and 9 UV observations, SPICAM (SPectroscopy for the Investigation of the Characteristics of the Atmosphere of Mars) on-board Mars Express (MEX) is the first instrument dedicated for the aeronomical studies of Mars. SPICAM has broaden our understanding about the Martian dayglow. Emissions observed by SPICAM in UV dayglow are H Lyman-α emission at 121.6 nm, the atomic oxygen emissions at 130.4 and 297.2 nm, the Cameron band ($a^3\Pi - X^1\Sigma^+$) and fourth positive band ($A^1\Pi - X^1\Sigma^+$) of CO, and ultraviolet doublet band ($B^2\Sigma^+ - X^2\Pi$) emissions of CO_2^+ (cf. Leblanc et al., 2006; Chaufray et al., 2008). These emission features are similar to those observed by Mariner 6, 7, and 9 but with better sensitivity, and spatial and temporal coverage. SPICAM has observed these dayglow emissions on Mars throughout the Martian year and showed the effect of solar zenith angle (SZA), seasonal variation, and Martian dust storms on the dayglow emissions (Leblanc et al., 2006, 2007; Shematovich et al., 2008; Simon et al., 2009; Cox et al., 2010). SPICAM also provided first observation of N_2 UV emissions in Martian dayglow (Leblanc et al., 2006, 2007). N_2 Vegard-Kaplan VK (0, 5) and (0, 6) band emissions at 260.4 nm and 276.2 nm, respectively, have been observed; N_2 VK (0, 7) emission at 293.7 nm has also been reported, but it has large uncertainty (Leblanc et al., 2007). The detailed model of N_2 dayglow emissions on Mars is presented elsewhere (Jain and Bhardwaj, 2011).

Several theoretical studies have been made for the dayglow emissions on Mars (Fox and Dalgarno, 1979; Mantas and Hanson, 1979; Conway, 1981; Shematovich et al., 2008; Simon et al., 2009). First detailed calculation of dayglow emission on Mars was carried out by Fox and Dalgarno (1979). Calculated overhead intensities of CO Cameron and CO_2^+ UV doublet bands were 49 kR and 12 kR, respectively, for the low solar activity condition similar to Viking landing (Fox and Dalgarno, 1979). Simon et al. (2009) used Trans-Mars model to calculate limb intensities of Cameron and CO_2^+ UV doublet emissions for low solar activity condition (similar to Viking landing) and compared them with SPICAM-observations. Their calculated intensities are higher by ∼25% than the observation. Simon et al. (2009) had to reduce the Viking CO_2 density in the model atmosphere by a factor of 3 to bring the altitude of peak emission in agreement with the observation.

Seasonal effects on intensities of Cameron and UV doublet bands have been observed by SPICAM (Simon et al., 2009; Cox et al., 2010). Cox et al. (2010) have presented a statistical analysis of Cameron band and UV doublet emissions, peak altitude of emissions, and ratios between UV doublet and Cameron band. Averaged peak emission brightness (altitude of peak emission) observed by Cox et al. (2010) for CO Cameron and UV doublet bands are 118 ± 33 kR (121 ± 6.5 km) and 21.6 ± 7.2 kR (119.1 ± 7.0 km), respectively. They also presented observations for one particular season, solar longitude (Ls) = 90 to 180°, and compared observational data with model calculations based on Monte Carlo code, which has been used also by Shematovich et al. (2008) for the Martian dayglow studies.

Modelling of CO Cameron and CO_2^+ UV doublet dayglow emissions requires a sophisticated input solar EUV (∼50 to 1000 Å) flux, which is a fundamental parameter to model physics, chemistry and dynamics of the upper atmosphere of planets. Since observations of solar EUV irradiance are not frequent and generally not available simultaneously with the observation for the upper atmospheric studies, the solar EUV flux model become important for modelling of aeronomical quantities in planetary atmospheres. Generally, solar EUV flux models are bin-averaged into numbers of wavelength bands and important solar emission lines appropriate for the calculation of photoionization and photoelectron impact production rates. Characterisation of the solar EUV flux for use in aeronomical and ionospheric studies were developed during the seventies based

on the Atmospheric Explorer-E (AE-E) data (Hinteregger, 1976; Hinteregger et al., 1981; Torr and Torr, 1985). Two AE-E reference spectra SC#21REF and F79050N have been published by Torr and Torr (1985) at 37 wavelength bins for solar minimum and maximum conditions, respectively. Later, based on the measured photoelectron flux, the short wavelength fluxes were increased by Richards et al. (1994), and they incorporated modified F74113 solar EUV flux in their EUVAC model. Detailed discussion on the development of solar EUV flux models is beyond the scope of this study; Lean (1990), Richards et al. (1994), and Lean et al. (2011) have provided reviews on solar EUV flux models.

For a given solar activity there are significant differences between the EUV fluxes reproduced by different solar flux models. These models are based on the different input parameters and proxies, e.g., solar 10.7 cm radio flux (henceforth referred to as solar F10.7) is used as the measure of solar activity, and used for parametrization of solar EUV flux models (Richards et al., 1994; Tobiska and Barth, 1990). EUVAC model of Richards et al. (1994) is based on solar F10.7 and its 81-day average and also on the F74113 solar flux (in the EUVAC model, the F74113 flux below 250 Å, and below 150 Å, are doubled and tripled, respectively). SOLAR2000 model of Tobiska et al. (2000) is based on measured solar flux irradiance and various proxies and provides solar flux from X-rays to infrared wavelengths, i.e., 1–1000000 Å.

Different solar EUV flux models have been used to study the solar radiation interaction with upper atmosphere of Mars. Presently, SOLAR2000 (S2K) model of Tobiska (2004) and EUVAC model of Richards et al. (1994) are commonly used solar EUV flux models in aeronomical studies of Mars; *e.g.*, Simon et al. (2009) and Huestis et al. (2010) have used EUVAC model, while Shematovich et al. (2008) and Cox et al. (2010) have used S2K model for the dayglow calculations on Mars.

Fox et al. (1996) have studied the effect of different solar EUV flux models on calculated electron densities for low and high solar activity conditions. They have used 85315 and 79050 solar fluxes of Tobiska (1991) and SC#21REF and F79050N AE-E reference solar spectra of Hinteregger (Torr et al., 1979) for low and high solar activity conditions, respectively. Fox et al. (1996) found that due to smaller fluxes at short wavelength range (18–200 Å) in Hinteregger spectra, lower peak in electron density profile is significantly reduced (30–35%) compared to that calculated using solar fluxes of Tobiska (1991). Buonsanto et al. (1995) calculated ionospheric electron density using EUVAC model of Richards et al. (1994) and EUV94X solar flux model of Tobiska (1994). They found that photoionization rate in F2 region calculated by using EUV94X model is larger than that calculated using EUVAC model due to the large EUV fluxes in 300–1050 Å wavelength range in EUV94X solar flux model. Recently, Jain and Bhardwaj (2011) have studied the effect of solar EUV flux models on N_2 VK band intensities in Martian dayglow and showed that EUV flux models does affect the N_2 dayglow emissions. Similar conclusion have been drawn for N_2 dayglow emission on Venus (Bhardwaj and Jain, 2011)

The aim of the present study is to calculate the impact of solar EUV flux models on CO Cameron band and CO_2^+ UV doublet band intensities in Martian dayglow. We have used 37 bin EUVAC model of Richards et al. (1994) and S2K version 2.36 of Tobiska (2004) as the solar EUV fluxes. In these models, bins consist of band of 50 Å width each and few prominent solar EUV lines, and are sufficient for the modelling of photoionization and photoelectron flux calculations (Richards et al., 1994; Simon et al., 2009). Photoelectron flux, volume excitation rates and overhead intensities are calculated using both the solar EUV flux models for low, moderate, and high solar activity conditions. Line of sight intensities for Cameron band and UV doublet emissions are calculated and compared with the latest observations by SPICAM instrument.

2 Model

Model atmosphere consists of five gases (CO_2, N_2, CO, O, and O_2). Model atmosphere for solar minimum condition is taken from the Mars Thermospheric General Circulation Model (MTGCM) (Bougher et al., 1999, 2000, 2004). Model atmosphere for high solar activity is taken from Fox (2004). Photoabsorption and photoionization cross sections for gases considered in the present study are taken from Schunk and Nagy (2000), and branching ratios for ionization in different states are taken from Avakyan et al. (1998).

Production mechanisms for CO($a^3\Pi$) are photon and electron impact dissociative excitation of CO_2, electron dis-

sociative recombination of CO_2^+, and electron impact excitation of CO. Since $X^1\Sigma^+ \rightarrow a^3\Pi$ is a forbidden transition, resonance fluorescence of CO is not an effective excitation mechanism. CO($a^3\Pi$) is a metastable state; Lawrence (1972) has measured its lifetime as 7.5 ± 1 ms, consistent with the measurement of Johnson (1972). Individual band lifetime can vary, e.g., lifetime of CO($a^3\Pi$) $\nu = 0$ level is around 3 ms (Gilijamse et al., 2007; Jongma et al., 1997). Due to its long lifetime, cross section for the production of Cameron bands due to electron impact dissociation of CO_2 is difficult to measure in the laboratory. Overall, Cameron band cross section can have an uncertainty of a factor of 2 (Bhardwaj and Jain, 2009). Ajello (1971) reported relative magnitudes of the cross section for the (0, 1) band at 215.8 nm. Erdman and Zipf (1983) estimated the total Cameron band emission cross section of 2.4×10^{-16} cm^2 at 80 eV, whereas Ajello estimated a value of 7.1×10^{-17} cm^2 at 80 eV. Bhardwaj and Jain (2009) have fitted the e-CO_2 cross sections producing CO Cameron band based on the estimated value of Erdman and Zipf (1983). In our study cross section for Cameron band production due to electron impact on CO_2 is taken from Bhardwaj and Jain (2009). Cross section for photodissociation of CO_2 producing CO($a^3\Pi$) is taken from Lawrence (1972). To calculate the production rate of CO($a^3\Pi$) due to dissociative electron recombination process we have calculated the density of electron and major ions by including ion-neutral chemistry in the model. The coupled chemistry model is similar to that adopted in our other studies (Bhardwaj et al., 1996; Bhardwaj, 1999; Haider and Bhardwaj, 2005). Rate coefficients for ion-neutral reactions are taken from Fox and Sung (2001). Recently, Seiersen et al. (2003) have measured recombination rates for the e-CO_2^+ collision, with yield of 0.87 for the channel producing CO of which CO($a^3\Pi$) production yield is 0.29 (Skrzypkowski et al., 1998; Rosati et al., 2003). Ion and electron temperatures are taken from Fox (2009). Ion and electron densities are calculated under steady state photochemical equilibrium. To calculate the density of CO($a^3\Pi$) we have also included various sources of loss of CO($a^3\Pi$) in our coupled chemistry model, which are given in Table 1.

Major production sources of CO_2^+ in B state are photon and electron impact ionization of CO_2. Cross section for the formation of $CO_2^+(B^2\Sigma_u^+)$ state due to electron impact ionization of CO_2 is taken from Itikawa (2002), and cross section due to photoionization of CO_2 is based on the branching ratio taken from Avakyan et al. (1998). For other gases electron impact cross sections have been taken from Jackman et al. (1977).

Solar EUV flux has been taken at 1 AU (based on solar F10.7 at 1 AU as seen from the Mars, taking the Sun-Earth-Mars angle into consideration) and then scaled to the Sun-Mars distance. Fig. 1 shows the output of EUVAC and S2K solar EUV flux models for both solar minimum (20 July 1976) and solar maximum (2 August 1969) conditions at 1 AU. There are substantial differences in the solar EUV fluxes of EUVAC and S2K models; moreover, these differences are not similar in solar minimum and maximum conditions. In both, solar minimum and maximum conditions, solar flux in bands is higher in S2K than in EUVAC over the entire range of wavelengths, except for bins below 250 Å (150 Å for solar minimum condition), whereas solar flux at lines is higher in EUVAC model for entire wavelength range. Overall higher solar fluxes above 250 Å in S2K cause more photoionization. Higher photon fluxes below 250 Å (during solar maximum condition) in EUVAC produce more higher energy electrons in the Martian atmosphere causing secondary ionizations (cf. Fig. 2) that can compensate for the higher photoionization in S2K model. One big difference between solar EUV fluxes of S2K and EUVAC models is the solar flux at bin containing 1026 Å H Ly-β line, which in both solar minimum and maximum conditions is around an order of magnitude higher in S2K compare to EUVAC solar flux model (cf. Fig. 1). Flux at these wavelengths does not contribute to the photoionization, but are very important for dissociative excitation processes. Cross section for the photodissociation of CO_2 producing Cameron band lies in longer (700–1080 Å) wavelength regime (Lawrence, 1972). Hence, yield of photodissociation excitation of CO_2 producing CO($a^3\Pi$) state would be larger when S2K solar EUV flux model is used.

To calculate the photon degradation and generation of photoelectrons in the atmosphere of Mars, we have used Lambert-Beer law. Solar zenith angle (SZA) is 45° unless mentioned otherwise in the text. Photoelectron energy degradation and production rates of excitation of CO Cameron band and CO_2^+ UV doublet band in the Martian atmosphere are calculated using Analytical Yield Spectrum (AYS) technique, which is based on the Monte Carlo model

(cf. Singhal and Bhardwaj, 1991; Bhardwaj and Singhal, 1993; Bhardwaj and Michael, 1999a,b; Bhardwaj and Jain, 2009). Details of calculation of photoelectron production rates and photoelectron flux have given in our earlier papers (Bhardwaj et al., 1990; Bhardwaj, 2003; Michael and Bhardwaj, 1997; Jain and Bhardwaj, 2011; Bhardwaj and Jain, 2011).

Below 70 eV, photoelectron flux calculated using S2K is higher compared to that calculated using EUVAC model for low solar activity condition (Fig. 2). Above 70 eV, photoelectron flux calculated using EUVAC model is higher than that calculated using S2K model due to the larger solar EUV fluxes at shorter wavelength (< 200 Å) in EUVAC model (cf. Fig. 1). During solar maximum condition photoelectron fluxes calculated by using EUVAC model is higher than that calculated using S2K model (cf. Fig. 2) due to higher solar EUV flux at wavelength below 250 Å in EUVAC model. During solar minimum, except at peaks and energies above 70 eV, photoelectron flux calculated using S2K model is around 1.4 times higher than that calculated using EUVAC model. During solar maximum condition photoelectron flux calculated using EUVAC model are higher than that calculated using S2K model. Photoelectron fluxes calculated using both solar EUV flux models are similar in shape but peaks around 20–30 eV are more prominent in electron flux calculated using EUVAC due to the higher solar EUV flux at lines (e.g., He II Lyman-α line at 303.78 Å) in EUVAC model (Fig. 1). The peaks in the 20–30 eV region of the photoelectron flux arise due to the ionization of CO_2 in different ionization states by solar EUV flux at 303.78 line (Mantas and Hanson, 1979). Our calculated photoelectron fluxes are in good agreement with other model calculations (cf. Jain and Bhardwaj, 2011).

Volume excitation rate is calculated for important processes producing CO($a^3\Pi$) and $CO_2^+(B^2\Sigma_u^+)$ states using photoelectron flux as

$$V_i(Z) = n(Z) \int_{E_{th}}^{E} \phi(Z,E)\sigma_i(E)dE, \qquad (1)$$

where $n(Z)$ is the density at altitude Z, $\sigma_i(E)$ is the electron impact cross section for i^{th} process, for which threshold is E_{th}, and $\phi(Z,E)$ is the photoelectron flux.

3 Results and discussion

3.1 Low solar activity condition

We run the model for low solar activity condition (similar to Viking landing), and calculated results are compared with those of Fox and Dalgarno (1979) by taking the similar model atmosphere. Model atmosphere is based on density data derived from Viking 1 (Nier and McElroy, 1976). The Sun-Mars distance D_{S-M} = 1.64 AU and solar zenith angle is taken as 45°.

Fig. 3 shows the calculated densities of CO_2^+ and O_2^+ in the Martian upper atmosphere. The density of CO_2^+ around peak and above calculated using S2K model is ∼30% higher than that calculated using EUVAC, which is due to higher production rate of CO_2^+ when S2K model is used. Below 120 km, ion densities calculated by using EUVAC model are higher due to the higher photoelectron fluxes above 70 eV (cf. Fig. 2). There is a small discontinuity in the density of O_2^+ ion around 180 km, which is due to the sudden change in the electron temperature at 180 km (see Fig. 2 of Fox, 2009). Our calculated ion densities are consistent with calculations of Fox (2004).

Fig. 4 (upper panel) shows the profiles of production mechanisms of CO($a^3\Pi$) calculated using EUVAC and S2K solar EUV flux models. Around the peak of CO($a^3\Pi$) production, the major source is photoelectron impact dissociation of CO_2, while at higher altitudes photodissociation excitation of CO_2 takes over. Dissociative recombination is about 13%, while photoelectron excitation of CO contribute about 3% to the total Cameron band excitation at the peak. The shape of volume excitation rate (VER) profiles and the altitude at the peak remain the same for all processes for the two solar flux models. However, the magnitude of VERs calculated using S2K model are about 40% higher than those calculated using EUVAC model. Contribution of electron impact dissociation of CO_2 producing CO($a^3\Pi$) is higher in our studies than that in Fox and Dalgarno (1979). This is due to the higher value of CO($a^3\Pi$) production cross section in e-CO_2 collision used in the present study (having the value of 1×10^{-16} cm^2 at 27 eV); Fox and Dalgarno (1979) used the cross section derived from Freund (1971) (having the value of 4×10^{-17} cm^2 at 27 eV). Due to larger photon flux at longer (700–1050 Å) wavelengths (region where photodissociation of CO_2 becomes important) in S2K model compared to EUVAC

model (cf. Fig. 1), CO($a^3\Pi$) production due to photodissociative excitation is higher by ∼50% when S2K model is used. Production rates of CO Cameron band for different processes calculated at the peak along with the peak altitude are given in Table 2.

It is also clear from upper panel of Fig. 4 that the altitude where the photodissociation of CO_2 takes over electron impact dissociation of CO_2 in CO($a^3\Pi$) formation is slightly higher when EUVAC model is used (167 km for EUVAC and 160 km for S2K solar flux model). In our model calculations, as well as in the work of Simon et al. (2009), photodissociation process becomes the major source at higher altitudes (> 160 km) and is a factor of 2 higher than the electron impact dissociation of CO_2.

For the CO_2^+ UV doublet band, we have considered only photoionization and electron impact ionization of CO_2 producing CO_2^+ in the $B^3\Sigma_u^+$ state. Contribution of solar fluorescent scattering is very small, less than 10% (cf. Fox and Dalgarno, 1979), and hence it is not taken into account in the present study. While calculating the emission from CO_2^+ UV doublet, we have assumed 50% crossover from B to A state (Fox and Dalgarno, 1979). Fig. 4 (bottom panel) shows the production rates for CO_2^+ in B state. Production of $CO_2^+(B^2\Sigma_u^+)$ due to photoionization of CO_2 is about a factor of 3–4 higher than due to photoelectron impact ionization. Here also we find that production rates calculated using S2K are higher than those calculated using EUVAC flux by about 50%, but peak altitude remains the same in both cases. Production rates calculated at peak along with peak altitude for CO_2^+ UV doublet band are given in Table 2.

Volume emission rates are height-integrated to calculate overhead intensities, which are presented in Table 3 for CO Cameron and UV doublet bands. For Cameron band, contribution of e-CO_2 process is maximum (64%) followed by photodissociation of CO_2 (21%). Contributions of dissociative recombination and e-CO process are around 10% and 3%, respectively. For UV doublet band, the major contribution is coming from photoionization of CO_2 (80%), the rest is due to electron impact ionization of CO_2.

To compare the model output with observed emissions we have integrated volume emission rates along the line of sight. Limb intensity at each tangent point is calculated as

$$I = 2\int_0^\infty \mathrm{V}(r)dr, \tag{2}$$

where r is abscissa along the horizontal line of sight, and V(r) is the volume emission rate (in cm^{-3} s^{-1}) at a particular emission point r. The factor of 2 multiplication comes due to symmetry along the line of sight with respect to the tangent point. While calculating limb intensity we assumed that the emission rate is constant along local longitude/latitude. For emissions considered in the present study the effect of absorption in the atmosphere is found to be negligible.

Fig. 5 shows the calculated limb profiles of the CO Cameron and CO_2^+ UV doublet bands along with the SPICAM-observed limb intensity taken from Simon et al. (2009). Observed values are averaged over for the orbits close to Viking 1 condition (Ls∼100–140°), low solar activity, and for SZA=45°. Below 100 km there is a sudden increase in the observed intensity of CO_2^+ UV doublet band, which, according to Simon et al. (2009), is due to the very significant solar contamination below 100 km. Limb intensities calculated using S2K flux are ∼40–50% higher than those calculated using EUVAC: clearly showing the effect of input solar EUV flux on the calculated intensities. Magnitude of the calculated limb intensity of UV doublet band is in agreement with the observation, but for CO Cameron band calculated intensity is higher than the observed profile. For both bands, the calculated intensity profile peaks at higher (∼5 km) altitude in comparison with the observation–indicating a denser neutral atmosphere in our model.

The dashed curves in Fig. 5 show intensities calculated after reducing the CO_2 density by a factor of 1.5; a good agreement in the altitude of peak emission is seen between calculated and observed limb profiles. Though the reduction in CO_2 density shifted the altitude of peak emission downwards, the magnitude of calculated Cameron band intensity is still larger than the intensity measured by SPICAM. As pointed out in Section 2, the e-CO_2 cross sections producing Cameron band are uncertain by a factor of ∼2. The calculated limb intensity profile for reduced e-CO_2 cross section by a factor of 2 is also shown in Fig. 5. Cameron band intensities obtained after reducing

the density and cross section are in relatively close agreement with the observed values. In the model calculations of Simon et al. (2009) also the Cameron band intensity and its peak emission altitude were higher than the SPICAM observed values. They have to reduced the density of CO_2 by a factor of 3 and e-CO_2 Cameron production cross section by a factor of 2 to bring their calculated intensity profile in agreement with the SPICAM observation.

3.2 SPICAM observations

Leblanc et al. (2006) have presented detailed analysis of SPICAM data during the period October 2004 to March 2005, spanning the solar longitude (Ls) from 101° to 171°. They divided the total data set in two periods of solar longitude: first, Ls = 101° to 130°, and second, Ls = 139° to 171° (cf. Table 2 of Leblanc et al., 2006). Leblanc et al. found that the altitude of peak emission for CO_2^+ UV doublet and CO Cameron bands is around 10 km higher for Ls > 138° (122.5 km and 132.5 km for UV doublet and Cameron bands, respectively) compared to Ls < 130° (112.5 km and 117.5 km, for the same emissions). Leblanc et al. (2006) could not provide the reason for the higher altitude of peak emission for Ls > 130° observations. Later, Forget et al. (2009) derived neutral densities in Martian upper atmosphere using the SPICAM instrument in stellar occultation mode for the same observation period. Forget et al. (2009) found that their is a sudden increase in the CO_2 density in the Martian upper atmosphere for Ls ∼ 130°–140°, which they attributed to a dust storm. Dust storm can heat the lower atmosphere and thus increase the densities at higher altitudes, which could explain the higher altitude for peak emission observed by the SPICAM for Ls > 130° observations. Increase in the altitude of peak intensity of dayglow emissions clearly shows the effect of dust storms on Martian dayglow emissions.

Comparisons of SPICAM observations with model calculated dayglow emissions have been performed by Shematovich et al. (2008), Simon et al. (2009), and Cox et al. (2010). Simon et al. (2009) have used one dimensional Trans-Mars model with EUVAC solar flux model, whereas Shematovich et al. (2008) and Cox et al. (2010) have used Monte Carlo model with S2K solar flux. In the present study, we have taken both EUVAC and S2K models and have calculated the Cameron band and UV doublet band emissions using the Analytical Yield Spectrum method; the results are compared with the SPICAM observations.

3.2.1 First Case (Ls < 130°)

To model the SPICAM observations for Ls < 130° the model atmosphere is based on MTGCM of Bougher et al. (1999) (taken from Shematovich et al., 2008). Calculations are made for MEX orbit no. 983 (24 Oct. 2004) when D_{S-M} = 1.64 AU, F10.7 = 87.7 (F10.7A = 107.3).

Fig. 6 (upper panel) shows the volume excitation rate of CO($a^3\Pi$). The total VER calculated using S2K flux is only slightly higher than that obtained using EUVAC flux. However, the production rate due to photodissociative excitation of CO_2 is around 50% higher when S2K model is used. Another interesting feature is the dissociative recombination (DR) process, whose contribution is ∼18% in the total intensity, roughly equal to the photodissociative excitation process (DR contribution is even higher than photodissociative excitation around production peak when EUVAC model is used), and it is significantly higher than compared to the DR process in Viking condition case (see Table 3). This is due to the higher density of CO_2^+ ion compared to Viking condition (see Fig. 3). Leblanc et al. (2006) mentioned that higher values of CO_2^+ can contribute up to 30% to the Cameron band production depending on the solar zenith angle. To account for DR in Cameron band production, Shematovich et al. (2008) and Cox et al. (2010) have taken CO_2^+ and electron densities from Fox (2004) for low solar activity condition. Since SPICAM observations are made during moderate solar activity condition, the contribution of DR in Cameron band production would be lower in their calculations.

Fig. 6 (bottom panel) shows the production rates of CO_2^+ UV doublet band. Total rate calculated using both solar flux models is peaking at same altitude (∼125 km), but total production rate calculated using S2K model is higher (around 10%) than that calculated using EUVAC model.

Table 3 shows the overhead intensities of CO Cameron and CO_2^+ UV doublet bands calculated using both EUVAC and S2K solar flux models. Contribution of different processes in Cameron band production is slightly different than that in the low solar activity condition. Contribution from CO_2 photodissociation is slightly reduced (17%, 21% when S2K model is used), while dissociative recombination

contribution is increased (∼18%). Contribution of e-CO_2 and e-CO processes remains almost same; 61 (64%) and 4 (4%), respectively, when calculated using EUVAC (S2K) model. For UV doublet band photoionization of CO_2 remains the dominant process contributing around 80% to the total overhead intensity.

We have also calculated overhead intensities of major vibrational bands of Cameron system, which have been observed in Martian dayglow, using Frank-Condon factors from Halmann et al. (1966) and branching ratio from Conway (1981). Table 4 shows the calculated overhead intensities of major vibrational bands of CO Cameron band system. Contribution of major vibrational bands to the total overhead Cameron band intensity is around 10, 10, 16, and 8% for (0, 0), (0, 1), (1, 0), and (2, 0) bands, respectively.

Fig. 7 shows the limb intensity profiles of Cameron and CO_2^+ UV doublet bands. SPICAM-observed intensities of Cameron and UV doublet bands averaged over Ls = 100–130° observations (Leblanc et al., 2006) are also shown in the Fig. 7. Limb intensities of CO_2^+ UV doublet and Cameron bands calculated by using S2K model are ∼6% and ∼15%, respectively, higher compared to those obtained using EUVAC model. Calculated intensities for both solar flux models are higher than the SPICAM-observed values. In analogy to the Viking case, we reduced the e-CO_2 cross sections producing Cameron band. The resulting intensity profile (also shown in Fig. 7) is still higher than the observation around emission peak. Calculated intensity of CO_2^+ UV doublet band is also higher near the peak emission than the observed intensity. Altitude of the calculated intensity for both CO Cameron and UV doublet bands peaks ∼2 to 3 km higher than the observations, which is well within the observational uncertainties. Line of sight intensity of different vibrational transitions of Cameron band at the altitude of peak emission, which is ∼120 km for first case, are shown in Table 4.

Fig. 8 shows the calculated intensity ratio of UV doublet to Cameron band along with the observed ratio derived from SPICAM observations (Leblanc et al., 2006). At lower altitudes calculated ratio is in agreement with observation (∼0.18). The ratio remains almost constant up to ∼120 km (where Cameron band and UV doublet emission peaks), starts gradually decreasing with altitude and becomes almost constant after 150 km. The observed ratio decreases almost monotonically from 100 km all the way to 180 km. Leblanc et al. (2006) have not found any dependence of SZA on the UV doublet to Cameron band intensity ratios, though they have observed a weak dependence of this intensity ratio on the solar activity. From the observed intensity ratio profile it is clear that in upper atmosphere Cameron band intensity is increasing steadily compare to UV doublet band, which indicates a difference in the source of production of Cameron band and UV doublet band. That source could be the dissociative recombination process which is sensitive to the density of CO_2^+ ion (as shown in the Fig. 3). Loss of CO_2^+ ions at higher altitudes (> 200) can reduce the intensity of UV doublet and hence decreases the intensity ratio value.

3.2.2 Second Case (Ls > 130°)

As discussed earlier, due to dust storm during SPICAM observations for Ls greater than 130°, atmospheric densities were higher resulting in altitude of peak emission shifting to higher altitudes (∼132.5 km for Cameron band emission). For Mariner 6 and 7 observations the intensity of CO Cameron band peaked at altitude of ∼133 km. Mariner observations were carried out during solar maximum condition (F10.7 ∼ 180), whereas SPICAM observations are made during moderate solar activity condition. To model dayglow emissions for Ls > 130°, we have made calculation for MEX orbit 1426 (26 Feb. 2005), taking model atmosphere from Fox (2004) for high solar activity condition. Sun-Mars distance is 1.5 AU, F10.7 = 98 (F10.7A = 97). The EUV flux at 1 AU calculated using EUVAC model remains the same for first (Ls < 130°) and second (Ls >130°) cases. This is because in the EUVAC model average of F10.7 and F10.7A (81-day average) is used to scale the solar flux, and on both days average of F10.7 and F10.7A does not change (it is 97.5 on both days), although the F10.7 flux increased by 10 unit. S2K model does not depend on the F10.7 alone, but on other proxies also (Tobiska, 2004), hence flux calculated using S2K model is different on the two days.

Fig. 9 (upper panel) shows the VER of CO($a^3\Pi$) calculated using S2K and EUVAC models. Total VER calculated using S2K is about 17% higher than that calculated using EUVAC model. Major differences are in the CO($a^3\Pi$) production due to dissociative excitation of CO_2 by photon and electron impact, which are more than 50% and 10%

higher, respectively, when S2K model is used. Total production rate of Cameron band (calculated using EUVAC model) maximises at an altitude of 134 km with a value of about 3328 cm^{-3} s^{-1}, which is around 10 km higher than that in the first case (Ls < 130°). Although production rate (3528 cm^{-3} s^{-1}) at peak altitude is higher in the first case, but at higher altitudes rate increases faster in the second (Ls > 130°) case, e.g., at 200 km, Cameron band production rate is 61 cm^{-3} s^{-1} in second case, whereas in first case it is only 3 cm^{-3} s^{-1}. In both, first and second cases, for EUVAC model, the altitude where photodissociation of CO_2 takes over electron impact dissociation of CO_2 is around 30% higher than that for S2K model.

Bottom panel of Fig. 9 shows production rates of CO_2^+ UV doublet band. Total excitation rate calculated using the S2K model is about 12% higher than that calculated using EUVAC model. Similar to the Cameron band, CO_2^+ UV doublet production rate at peak is lower than that in the first case, but at higher altitudes UV doublet production rate becomes higher in the second case. Table 3 shows the overhead intensities of Cameron and CO_2^+ UV doublet bands. Contribution of photodissociation of CO_2, e-CO_2, DR, and e-CO processes to the total Cameron band production is 16 (22%), 62 (57%), 11 (11%), and 9 (8%), respectively, when EUVAC (S2K) model is used.

Fig. 10 shows the calculated limb intensity of UV doublet and Cameron band along with SPICAM-observed intensities of Cameron band and CO_2^+ doublet band for MEX orbit 1426 on 26 Feb. 2005 (Shematovich et al., 2008). Intensities calculated using S2K model are higher by ∼12–18% than those calculated using EUVAC model. Altitude of peak emission of calculated and observed intensity profiles is in good agreement with each other (e.g., ∼128 km for Cameron band) within the uncertainties of observations and model calculations. However, intensities calculated using both solar flux models are higher than the observations. Calculated intensities of CO Cameron band after reducing the e-CO_2 cross section by a factor of 2 are also shown in Fig. 10, which is in good agreement with the observed values. However, the calculated intensity of UV doublet band is 20–30% higher than the SPICAM-observed values. Uncertainties in photoionization cross sections for the production of $CO_2^+(B^2\Sigma_u^+)$ can also be one of reasons for the differences between observed and calculated intensity of $CO_2^+(B^2\Sigma_u^+)$ UV doublet emission.

In our calculation (using EUVAC model and reduced e-CO_2 cross section for Cameron band production), peak brightness of Cameron band is 249 (255) kR with peak located at 120 (128) km in first (second) case. For CO_2^+ UV doublet band, peak brightness is 31 (33) kR with peak located at 119 (127) km in first (second) case. Altitude of peak brightness remains the same when S2K model is used but intensities of Cameron and CO_2^+ UV doublet bands for first (second) case are about a factor of 1.1 (1.18) and 1.07 (1.11), respectively, higher than that calculated using EUVAC model.

3.3 Solar Maximum (Mariner Observations)

First dayglow measurements on Mars were carried out by Mariner series of spacecraft. Mariner 6 and 7 observations were taken during the solar maximum conditions (July-August, 1969; F10.7 = 186 at 1 AU), and are the only Martian dayglow observations so far taken during the solar maximum condition. Mars was also at perihelion (distance between Sun and Mars was around 1.42 AU) during Mariner observations. We run our model for the condition similar to the Mariner observation. Model atmosphere for solar maximum condition is taken from Fox (2004).

Fig. 1 (bottom panel) shows the solar EUV flux during Mariner observations (2 Aug. 1969, F10.7 = 180) from EUVAC and S2K models. As discussed in Section 2, overall the solar EUV flux is higher in S2K model, except at wavelengths below 250 Å where EUVAC flux is larger. Fig. 2 (bottom panel) shows photoelectron fluxes calculated at different heights in solar maximum condition using both solar flux models. Unlike in the solar minimum condition, the ratio of photoelectron flux calculated using S2K to that of EUVAC is less than 1 at most of the energies. At electron energies below 30 eV, fluxes calculated using S2K and EUVAC models are almost equal at altitudes of 130 and 160 km. Above 30 eV, photoelectron fluxes calculated using EUVAC model are higher than those calculated using S2K model. The higher photon fluxes in EUVAC model at shorter wavelengths below 250 Å [cf. Fig. 1] produce higher energy photoelectrons that can produce more secondary electron through ionization, and hence compensates for the higher solar EUV flux above 250 Å in the S2K model. Table 3 shows the calculated overhead intensities of Cameron band and UV doublet band using EUVAC and

S2K models. Cameron band production due to electron impact dissociation of CO_2 is higher when EUVAC model is used, which is due to the higher photoelectron fluxes. Contribution of photodissociation excitation calculated using S2K model is higher, due to higher EUV flux at longer wavelengths (specially flux in the 1000–1050 Å bin).

Fig. 11 (upper panel) shows the VER of CO($a^3\Pi$) for higher solar activity condition, calculated using EUVAC and S2K solar flux models. Due to the higher photoelectron flux, CO($a^3\Pi$) production due to e-CO_2, e-CO, and dissociative recombination are higher when EUVAC model is used. Photodissociative excitation of CO_2 producing Cameron band for S2K model is still higher by ∼50% than for EUVAC model, which is due to the higher EUV fluxes at longer wavelengths in the S2K model. Similar to that in the previous cases, the cross over point between photodissociation and electron impact dissociation of CO_2 forming CO($a^3\Pi$) occurs at higher altitude when EUVAC model is used. Bottom panel of Fig. 11 shows the production rates of CO_2^+ UV doublet band. Here also calculated values using EUVAC model is slightly higher than that calculated using S2K model.

During solar minimum condition total volume production rate of Cameron and UV doublet bands calculated using S2K model is higher than that calculated using EUVAC model, whereas in solar maximum it is vice-versa. Except photodissociation excitation process producing Cameron band, production rates due to other processes calculated by using EUVAC model are higher than that calculated by using S2K model. In both, solar minimum and maximum conditions, Cameron band production due to photodissociative excitation is about 50% higher, when S2K model is used.

Fig. 12 shows model intensities of Cameron band and CO_2^+(B – X) ultraviolet doublet band calculated using both EUVAC and S2K models at SZA = 45° along with intensities observed by Mariner 6 and 7. Limb intensities measured by Mariner 6 and 7 on Mars are at SZA = 27° and 0°, and at SZA = 44° and 0°, respectively. Calculated limb intensities using EUVAC model at SZA = 0° are also shown in the Fig. 12. Limb intensities calculated using EUVAC model are only slightly higher than those calculated using S2K model. There were no observations at emission peak for both Cameron band and CO_2^+(B – X) band. Below the emission peak, there are few observations for Cameron band, but ultraviolet doublet observations were not available. Solar zenith angle effect is clearly visible at altitudes below 150 km, where intensity is larger and emission peak shift deeper in the atmosphere for lower SZA. Calculated intensities of Cameron and UV doublet bands are lower than the observed values. Unlike previous cases, calculated intensities of Cameron and UV doublet band emissions at the altitude of peak emission are slightly lower than the observation. Stewart et al. (1972) has pointed out that due to calibration problem in Mariner 6 and 7 instrument the observed values can be higher. As in the previous cases a reduction in e-CO_2 cross section is required to get an agreement between observed and calculated intensity. Calculated intensity of Cameron band after reducing the e-CO_2 cross section by a factor of 2 is also shown in Figure 12 for SZA=0°.

3.4 CO($a^3\Pi$) density

Density of CO($a^3\Pi$) is calculated under photochemical equilibrium condition. Radiative decay is the dominant loss process of CO($a^3\Pi$), the contribution from other processes are negligible (cf. Bhardwaj and Raghuram, 2011). Fig. 3 shows the density of CO($a^3\Pi$) calculated using EUVAC and S2K EUV flux models for low solar activity condition. The calculated column density of CO($a^3\Pi$) molecule is 4.6×10^7 (6.5×10^7) cm^{-2} for the solar minimum condition using EUVAC (S2K) solar EUV flux model. Except in the solar maximum condition, density of CO($a^3\Pi$) molecule calculated using S2K model is higher than that calculated using EUVAC model. During solar maximum condition, CO($a^3\Pi$) density calculated using EUVAC model is slightly higher at peak (around 5%), but at altitudes above 140 km, density calculated using S2K model becomes higher (∼10% at 200 km).

The shape of the density of CO($a^3\Pi$) is similar to that of its production rate (cf. Fig. 4) since the main loss mechanism of CO($a^3\Pi$) is radiative decay whose value is independent of altitude. Hence, the density of CO($a^3\Pi$) in the Martian atmosphere can be represented by

$$[CO(a^3\Pi)] = \frac{[CO_2]\,(K_1 + K_2) + [CO_2^+]\,[n_e]\,K_3}{K_4} \quad (3)$$

where K_1, K_2, K_3, and K_4 are as described in Table 1. K_1 and K_2 are photodissociation rate and electron impact dissociation rate of CO_2, respectively, K_3 is dissociative

recombination, K_4 is radiative decay loss, and n_e is the electron density. The values of K_1 (photodissociation rate) in units of s^{-1} at the top of atmosphere in case of EUVAC (S2K) model are 7.5×10^{-8} (1.1×10^{-7}), 8.7×10^{-8} (1.3×10^{-7}), 1.03×10^{-7} (1.6×10^{-7}), and 1.5×10^{-7} (2.25×10^{-7}) in the solar minimum, first case, second case, and solar maximum, respectively.

4 Summary and Conclusion

Present study deals with the model calculations of CO Cameron band and CO_2^+ doublet ultraviolet emissions in Martian dayglow and the impact of solar EUV flux on the calculated intensities. Photoelectrons generated due to photoionization in the Martian atmosphere have been degraded in the atmosphere using Monte Carlo model–based Analytical Yield Spectrum technique. Emission rates of Cameron and CO_2^+ UV doublet bands due to photon and electron impact on CO_2 have been calculated using EUVAC and S2K solar EUV flux models. Densities of prominent ions and CO($a^3\Pi$) in Martian upper atmosphere are calculated under steady state photochemical equilibrium condition. Production rates of Cameron and CO_2^+ UV doublet bands are height-integrated to calculate overhead intensity and along the line of sight to obtain limb intensities. Limb intensities are compared with the SPICAM/Mars Express and UV spectrometer/Mariner observed intensities.

Due to higher EUV fluxes at longer (700–1050 Å) wavelengths in the S2K model, the contribution of photodissociation of CO_2 in producing Cameron band is about 50% higher in low as well as in high solar activity conditions. Variations in EUV fluxes at longer wavelengths from solar minimum to solar maximum are less prominent in the EUVAC solar EUV flux model compared to the S2K model.

For low solar activity condition, limb intensities of Cameron and CO_2^+ UV doublet bands around peak brightness calculated using S2K model are ∼30–40% higher than those calculated using EUVAC model. Comparison of calculated intensities has been made with the SPICAM-observed values for condition similar to the Viking. Intensities calculated using both S2K and EUVAC models are higher than the observed values. Calculated altitude of emission peak of CO Cameron and CO_2^+ UV doublet bands is also higher by ∼5 km than the observed value. A reduction in the e-CO_2 cross section forming Cameron band by a factor of 2 and the density of CO_2 in model atmosphere by a factor of 1.5 brings the calculated intensity (using EUVAC model) of Cameron band in close agreement with the SPICAM observation.

While modelling the recent observations made by SPICAM on-board Mars Express, we have taken two set of conditions with different model atmospheres and solar longitudes. In the first case, Ls < 130° (Ls = 100-130°), atmosphere is taken from Mars Thermospheric General Circulation model (Bougher et al., 1999, 2000, 2004) and calculations are made for the day 24 October 2004 with moderated solar activity flux (F10.7 = 88). Total intensities of CO Cameron and CO_2^+ UV doublet bands calculated using S2K model are around ∼6–15% higher than those calculated using EUVAC model. Contribution of CO_2 photodissociative excitation in Cameron band production is 50% higher when S2K model is used. Dissociative recombination of CO_2^+ is an important source of Cameron band in this case (cf. Fig. 6) due to higher densities of CO_2^+ ion (Fig. 3) compared to those calculated for low solar activity condition (Viking condition).

Calculated intensities of Cameron and UV doublet bands have been compared with the SPICAM-observed limb intensities. Intensities calculated using S2K and EUVAC solar flux models are higher than the observed values by a factor of 1.7 to 2 for Cameron and a factor of 1.4 for UV doublet bands (see Fig. 7). We found that altitude of peak emission of both Cameron and UV doublet bands are 2 to 3 km higher than observed profiles. This discrepancy in observed and calculated intensities and altitudes could be due to the fact that observed values are averaged over several days of observations while calculation are carried out for a particular day.

Due to the dust storm during Ls > 130°, observed emission peak is around 10 km higher for both Cameron and UV doublet compared with the SPICAM-observed values for MEX orbit 1426 on 26 Feb. 2005 (Shematovich et al., 2008). To model the emission during Ls > 130°, we have taken atmospheric model for solar maximum condition. Intensities calculated using the S2K solar flux model are ∼8–18% higher than those calculated using the EUVAC model. These calculated intensities are higher than the observed-averaged values by a factor of ∼2 for Cameron band and ∼50% for UV doublet band. The calculated intensity of Cameron band (after reducing the e-CO_2 cross sections by

a factor of 2) is in agreement with the observed values (Fig. 10).

In all three conditions discussed above, i.e., low solar activity (Viking), and first (Ls $< 130°$) and second (Ls $> 130°$) cases, calculated intensities of both Cameron and UV doublet bands are higher than observations. On an average, model values of Cox et al. (2010) for Cameron and CO_2^+ UV doublet bands are around a factor of 1.74 and 1.41, respectively, higher than the SPICAM observations. Simon et al. (2009) also found that their calculated intensities of Cameron and UV doublet bands are around 25% higher than the SPICAM-observed values. This shows that these discrepancies in the model and observed values are due the uncertainties in the input physical parameters in the model. Uncertainties in cross sections, namely, e-CO_2 cross section producing Cameron band and photoionization of CO_2 forming UV doublet band can be one of the causes of discrepancies in the model and observations.

Calculations are also made for the high solar (Mariner 6 and 7 observations) activity condition. Though the contribution of CO_2 photodissociative excitation in Cameron band production is higher when S2K model is used, but the total intensity of CO Cameron band calculated using the EUVAC model is slightly higher than that calculated using the S2K model. This is because of the higher photoelectron flux when EUVAC model is used (Fig. 2). The calculated intensities of both Cameron and UV doublet band are lower than the observed values (Fig. 12).

Following conclusion can be drawn from the present study:

1. Generally, solar EUV fluxes in bands are higher in S2K model except at few bands at shorter wavelength range (< 250 Å). Solar EUV fluxes at longer wavelengths are higher in S2K model, specially in the 1000-1050 Å bin, where flux is around an order of magnitude higher than the corresponding flux in EUVAC model. Solar EUV flux at lines is smaller in the S2K model compared to that in the EUVAC model.

2. Due to higher EUV flux at lines in the EUVAC model, peaks at 20–30 eV range in the photoelectron flux are more prominent when EUVAC model is used.

3. During high solar activity condition, calculated photoelectron fluxes are higher for EUVAC model due to higher EUV fluxes below 250 Å in the EUVAC model. Hence, intensities calculated using EUVAC model are higher by 5–10% than those calculated using S2K model.

4. During solar minimum condition, the Cameron and CO_2^+ UV doublet intensities calculated using S2K solar flux model are ∼30–40% higher than those calculated using the EUVAC model.

5. During both, solar minimum as well as maximum conditions, Cameron band production due to photodissociative excitation of CO_2 is about 50% higher when S2K solar EUV flux model is used.

6. Altitude of peak production rate of Cameron and CO_2^+ UV doublet bands is independent of solar EUV flux model used in the calculations. However, for the Cameron band the altitude where photodissociation of CO_2 takes over electron impact dissociation is higher in the EUVAC model compared to that in the S2K model.

7. Reduction in the e-CO_2 cross section producing Cameron band and photoionization cross section producing CO_2^+ UV doublet band is required to bring the model calculations in agreement with the observations.

8. For a given set of observation, and accounting for the uncertainties in the cross sections, intensities calculated using the EUVAC model are in better agreement with the observation than those calculated using the S2K model.

Simultaneous observation of solar EUV flux with dayglow measurements would be very helpful in improving our understanding of the processes that governs the dayglow emissions on Mars. More accurate measurements of cross sections for electron impact dissociation of CO_2 producing Cameron band and photoionization of CO_2 in B state are required for the better modelling of CO Cameron band and CO_2^+ UV doublet band in Martian atmosphere, as well as in other CO_2–containing atmospheres, like Venus and comets.

References

Ajello, J. M., 1971. Emission cross sections of CO_2 by electron impact in the interval 1260-4500 Å. J. Chem. Phys. 55, 3169 – 3177. doi:10.1063/1.1676564.

Avakyan, S. V., II'in, R. N., Lavrov, V. M., Ogurtsov, G. N., 1998. In: Avakyan, S. V. (Ed.), Collision Processes and Excitation of UV Emission from Planetary Atmospheric Gases: A Handbook of Cross Sections. Gordon and Breach science publishers.

Barth, C. A., Hord, C. W., Pearce, J. B., Kelly, K. K., Anderson, G. P., Stewart, A. I., 1971. Mariner 6 and 7 ultraviolet spectrometer experiment: Upper atmosphere data. J. Geophys. Res. 76, 2213 – 2227. doi:10.1029/JA076i010p02213.

Bhardwaj, A., 1999. On the role of solar EUV, photoelectrons, and auroral electrons in the chemistry of C(^{1}D) and the production of CI 1931 Å in the inner cometary coma: A case for comet P/Halley. J. Geophys. Res. 104, 1929 – 1942. doi:10.1029/1998JE900004.

Bhardwaj, A., 2003. On the solar EUV deposition in the inner comae of comets with large gas production rates. Geophys. Res. Lett. 30 (24), 2244. doi:10.1029/2003GL018495.

Bhardwaj, A., Haider, S. A., Singhal, R. P., 1990. Auroral and photoelectron fluxes in cometary ionospheres. Icarus 85, 216 – 228. doi:10.1016/0019-1035(90)90112-M.

Bhardwaj, A., Haider, S. A., Singhal, R. P., 1996. Production and emissions of atomic carbon and oxygen in the inner coma of comet 1P/Halley: role of electron impact. Icarus 120, 412 – 430. doi:10.1006/icar.1996.0061.

Bhardwaj, A., Jain, S. K., 2009. Monte Carlo model of electron energy degradation in a CO_2 atmosphere. J. Geophys. Res. 114. doi:10.1029/2009JA014298.

Bhardwaj, A., Jain, S. K., 2011. Calculations of N_2 triplet states vibrational populations and band emissions in venusian dayglow. Icarus . doi:10.1016/j.icarus.2011.05.026.

Bhardwaj, A., Michael, M., 1999a. Monte Carlo model for electron degradation in SO_2 gas: cross sections, yield spectra and efficiencies. J. Geophys. Res. 104 (10), 24713 – 24728. doi:10.1029/1999JA900283.

Bhardwaj, A., Michael, M., 1999b. On the excitation of Io's atmosphere by the photoelectrons: Application of the analytical yield spectrum of SO_2. Geophys. Res. Lett. 26, 393 – 396. doi:10.1029/1998GL900320.

Bhardwaj, A., Raghuram, S., 2011. Model for Cameron-band emission in comets: A case for the EPOXI mission target comet 103P/Hartley 2. Mon. Not. R. Astron. Soc. Lett. 412, L25 – L29. doi:10.1111/j.1745-3933.2010.00998.x.

Bhardwaj, A., Singhal, R. P., 1993. Optically thin H Lyman alpha production on outer planets: Low-energy proton acceleration in parallel electric fields and neutral H atom precipitation from ring current. J. Geophys. Res. 98 (A6), 9473 – 9481. doi:10.1029/92JA02400.

Bougher, S. W., Engel, S., Hinson, D. P., Murphy, J. R., 2004. MGS Radio Science electron density profiles: Interannual variability and implications for the Martian neutral atmosphere. J. Geophys. Res. 109. doi:10.1029/2003JE002154.

Bougher, S. W., Engel, S., Roble, R. G., Foster, B., 1999. Comparative terrestrial planet thermospheres: 2. Solar cycle variation of global structure and winds at equinox. J. Geophys. Res. 104, 16591 – 16611. doi:10.1029/1998JE001019.

Bougher, S. W., Engel, S., Roble, R. G., Foster, B., 2000. Comparative terrestrial planet thermospheres: 3. Solar cycle variation of global structure and winds at solstices. J. Geophys. Res. 105, 17669 – 17692. doi:10.1029/1999JE001232.

Buonsanto, M. J., Richards, P. G., Tobiska, W. K., Solomon, S. C., Tung, Y. .-K., Fennelly, J. A., 1995. Ionospheric Electron Densities Calculated Using Different EUV Flux Models and Cross Sections: Comparison with Radar Data. J. Geophys. Res. 100 (A8), 14569 – 14580. doi:10.1029/95JA00680.

Chaufray, J. Y., Bertaux, J. L., Leblanc, F., Quémerais, E., 2008. Observation of the hydrogen corona with SPICAM on Mars Express. Icarus 195 (2), 598 – 613. doi:10.1016/j.icarus.2008.01.009.

Conway, R. R., 1981. Spectroscopy of the Cameron bands in the Mars airglow. J. Geophys. Res. 86, 4767 – 4775. doi:10.1029/JA086iA06p04767.

Cox, C., Gérard, J. C., Hubert, B., Bertaux, J. L., Bougher, S. W., 2010. Mars ultraviolet dayglow variability: SPICAM observations and comparison with airglow model. J. Geophys. Res. 115. doi:10.1029/2009JE003504.

Erdman, P. W., Zipf, E. C., 1983. Electron-impact excitation of the Cameron system ($a^3\Pi \rightarrow X^1\Sigma$) of CO. Planet. Spece. Sci. 31, 317 – 321. doi:10.1016/0032-0633(83)90082-X.

Forget, F., Montmessin, F., Bertaux, J. L., Galindo, F. G., Lebonnois, S., Quémerais, E., Reberac, A., Dimarellis, E., Valverde, M. A. L., 2009. Density and temperatures of the upper Martian atmosphere measured by stellar occultations with Mars Express SPICAM. J. Geophys. Res. 114. doi:10.1029/2008JE003086.

Fox, J., Sung, K., 2001. Solar activity variations of the Venus thermosphere/ionosphere. J. Geophys. Res. 106 (A10), 21305 – 21335. doi:10.1029/2001JA000069.

Fox, J. L., 2004. Response of the Martian thermosphere/ionosphere to enhanced fluxes of solar soft X rays. J. Geophys. Res. 109. doi:10.1029/2004JA010380.

Fox, J. L., 2009. Morphology of the dayside ionosphere of Mars: Implications for ion outflows. J. Geophys. Res. 114. doi:10.1029/2009JE003432.

Fox, J. L., Dalgarno, A., 1979. Ionization, luminosity, and heating of the upper atmosphere of Mars. J. Geophys. Res. 84, 7315 – 7333. doi:10.1029/JA084iA12p07315.

Fox, J. L., Zhou, P., Bougher, S. W., 1996. The martian thermosphere/ionosphere at high and low solar activities. Adv. Space Res. 17 (11), 203 – 218. doi:10.1016/0273-1177(95)00751-Y.

Freund, R. S., 1971. Dissociation of CO_2 by electron impact with the formation of metastable CO($a^3\Pi$) and O(^{5}S). J. Chem. Phys. 55, 3569 – 3577. doi:10.1063/1.1676615.

Gilijamse, J. J., Hoekstra, S., Meek, S. A., Metsälä, M., van de Meerakker, S. Y. T., T, S. Y., Meijer, G., Groenenboom, G. C., C., G., 2007. The radiative lifetime of metastable CO ($a^3\Pi, \nu$=0). J. Chem. Phys. 127, 221102–4. doi:10.1063/1.2813888.

Haider, S. A., Bhardwaj, A., 2005. Radial distribution of production rates, loss rates and densities corresponding to ion masses $\leq$40 amu in the inner coma of Comet Halley: Composition and chemistry. Icarus 177, 196 – 216. doi:10.1016/j.icarus.2005.02.019.

Halmann, M, Laulicht, I, February 1966. Isotope effects on vibrational transition probabilities.IV. Electronic transitions of isotopic C_2, CO, CN, H_2, and CH molecules. Astrophysical Journal Supplement 12, 307 – 321. doi:10.1086/190130.

Hinteregger, E., 1976. EUV fluxes in the solar spectrum below 2000 Å. J . Atmos. Terr. Phys. 38, 791 – 806. doi:10.1016/0021-9169(76)90020-9.

Hinteregger, H. E., Fukui, K., Gilson, B. R., 1981. Observational, reference and model data on solar EUV, from measurements on AE-E. Geophys. Res. Lett. 8 (11), 1147 – 1150. doi:10.1029/GL008i011p01147.

Huestis, D. L., Slanger, T. G., Sharpee, B. D., Fox, J. L., 2010. Chemical origins of the Mars ultraviolet dayglow. Faraday Discussions 147, 307 – 322. doi:10.1039/c003456h.

Itikawa, Y., 2002. Cross sections for electron collisions with carbon dioxide. J. Phys. Chem. Ref. Data 31 (3), 749 – 767. doi:10.1063/1.1481879.

Jackman, C., Garvey, R., Green, A., 1977. Electron impact on atmospheric gases, I. Updated cross sections. J. Geophys. Res. 82 (32), 5081 – 5090. doi:10.1029/JA082i032p05081.

Jain, S. K., Bhardwaj, A., 2011. Model calculation of N_2 Vegard-Kaplan band emissions in Martian dayglow. J. Geophys. Res.doi:10.1029/2010JE003778.

Johnson, C. E., 1972. Lifetime of CO($a^3\Pi$) following electron impact dissociation of CO_2. J. Chem. Phys. 57 (1), 576 – 577. doi:10.1063/1.1678007.

Jongma, R. T., Berden, G., Meijer, G., Nov. 1997. State-specific lifetime determination of the $a^3\Pi$ state in CO. J. Chem. Phys. 107, 7034 – 7040. doi:10.1063/1.474946.

Lawrence, G., 1972. Photodissociation of CO_2 to produce CO($a^3\Pi$). J. Chem. Phys. 56, 3435 – 3442. doi:10.1063/1.1677717.

Lawrence, G. M., Jun. 1971. Quenching and radiation rates of CO ($a^3\Pi$). Chem. Phys. Lett. 9, 575 – 577. doi:10.1016/0009-2614(71)85130-8.

Lean, J., 1990. A comparison of models of the Sun?s extreme ultraviolet irradiance variations. J. Geophys. Res. 95 (A8), 11933 – 11944. doi:10.1029/JA095iA08p11933.

Lean, J. L., Woods, T. N., Eparvier, F. G., Meier, R. R., Strickland, D. J., Correira, J. T., Evans, J. S., 2011. Solar extreme ultraviolet irradiance: Present, past, and future. J. Geophys. Res. 116. doi:10.1029/2010JA015901.

Leblanc, F., Chaufray, J. Y., Bertaux, J. L., 2007. On Martian nitrogen dayglow emission observed by SPICAM UV spectrograph/Mars Express. Geophys. Res. Lett. 34. doi:10.1029/2006GL0284.

Leblanc, F., Chaufray, J. Y., Lilensten, J., Witasse, O., Bertaux, J.-L., 2006. Martian dayglow as seen by the SPICAM UV spectrograph on Mars Express. J. Geophys. Res. 111. doi:10.1029/2005JE002664.

Mantas, G. P., Hanson, W. B., 1979. Photoelectron fluxes in the Martian ionosphere. J. Geophys. Res. 84, 369 – 385. doi:10.1029/JA084iA02p00369.

Michael, M., Bhardwaj, A., 1997. On the dissociative ionization of SO_2 in the Io's atmosphere. Geophys. Res. Lett. 24, 1971 – 1974. doi:10.1029/97GL02056.

Nier, A. O., McElroy, M. B., 1976. Structure of the neutral upper atmosphere of Mars: Results from Viking 1 and Viking 2. Science 194, 1298 – 1300. doi:10.1126/science.194.4271.1298.

Richards, P. G., Fennelly, J. A., Torr, D. G., 1994. EUVAC: A solar EUV flux model for aeronomic calculations. J. Geophys. Res. 99, 8981 – 8992. doi:10.1029/94JA00518.

Rosati, R. E., Johnsen, R., Golde, M. F., 2003. Absolute yields of CO ($a'^3\Sigma^+$, $d^3\Delta_i$, $e^3\Sigma^-$) + O from the dissociative recombination of CO_2^+ ions with electrons. J. Chem. Phys. 119, 11630 – 11635. doi:10.1063/1.1623480.

Schunk, R. W., Nagy, A. F., 2000. Ionospheres: Physics, Plasma Physics, and Chemistry. Cambridge University Press.

Seiersen, K., Al-Khalili, A., Heber, O., Jensen, M. J., Nielsen, I. B., Pedersen, H. B., Safvan, C. P., Andersen, L. H., Aug 2003. Dissociative recombination of the cation and dication of CO_2. Phys. Rev. A 68 (2), 022708. doi:10.1103/PhysRevA.68.022708.

Shematovich, V. I., Bisikalo, D. V., Gérard, J.-C., Cox, C., Bougher, S. W., Leblanc, F., 2008. Monte Carlo model of electron transport for the calculation of Mars dayglow emissions. J. Geophys. Res. 113. doi:10.1029/2007JE002938.

Simon, C., Witasse, O., Leblanc, F., Gronoff, G., Bertaux, J.-L., 2009. Dayglow on Mars: Kinetic modeling with SPICAM UV limb data. Planetary Space Sci. 57, 1008 – 1021. doi:10.1016/j.pss.2008.08.012.

Singhal, R. P., Bhardwaj, A., 1991. Monte Carlo simulation of photoelectron energization in parallel electric fields: Electroglow on Uranus. J. Geophys. Res. 96, 15963 – 15972. doi:10.1029/90JA02749.

Skrzypkowski, M. P., Gougousi, T., Johnsen, R., Golde, M. F., May 1998. Measurement of the absolute yield of CO($a^3\Pi$)+O products in the dissociative recombination of CO_2^+ ions with electrons. J. Chem. Phys. 108, 8400 – 8407. doi:10.1063/1.476267.

Stewart, A. I., 1972. Mariner 6 and 7 ultraviolet spectrometer experiment: Implication of CO_2^+, CO, and O airglow. J. Geophys. Res. 77, 54 – 68. doi:10.1029/JA077i001p00054.

Stewart, A. I., Barth, C. A., Hord, C. W., Lane, A. L., 1972. Mariner 9 ultraviolet spectrometer experiment: Structure of Mars' upper atmosphere. Icarus 17 (2), 469 – 474. doi:10.1016/0019-1035(72)90012-7.

Tobiska, W., Barth, C., 1990. A Solar EUV Flux Model. J. Geophys. Res. 95 (A6), 8243 – 8251. doi:10.1029/JA095iA06p08243.

Tobiska, W. K., 1991. Revised Solar Extreme Ultraviolet Flux Model. J. Atm. Terr. Phys. 53, 1005 – 1018. doi:10.1016/0021-9169(91)90046-A.

Tobiska, W. K., 1994. Modeled soft X-ray solar irradiances. Solar Phys. 152, 207 – 215. doi:10.1007/BF01473206.

Tobiska, W. K., 2004. SOLAR2000 irradiances for climate change, aeronomy and space system engineering. Adv. Space Res. 34, 1736 – 1746. doi:10.1016/j.asr.2003.06.032.

Tobiska, W. K., Woods, T., Eparvier, F., Viereck, R., Floyd, L., Bouwer, D., Rottman, G., White, O. R., 2000. The SOLAR2000 empirical solar irradiance model and forecast tool. J. Atmos. Sol. Terr. Phys. 62, 1233 – 1250. doi:10.1016/S1364-6826(00)00070-5.

Torr, M. R., Torr, D. G., 1985. Ionization frequencies for solar cycle 21 - revised. J. Geophys.Res. 90, 6675 – 6678. doi:10.1029/JA090iA07p06675.

Torr, M. R., Torr, D. G. T., Hinteregger, H. E., 1979. Ionization freequencies for major thermospheric constituents as a function of solar cycle 21. Geophys. Res. Lett. 6, 771 – 774. doi:10.1029/GL006i010p00771.

Wysong, I. J., 2000. Measurement of quenching rates of $CO(a^3\Pi, \nu = 0)$ using laser pump-and-probe technique. Chem. Phys. Lett. 329 (1-2), 42 – 46. doi:10.1016/S0009-2614(00)00967-2.

Table 1: Major reactions for the production and loss of CO($a^3\Pi$).

Reaction	Rate ($cm^3\ s^{-1}$ or s^{-1})	Reference
$CO_2 + h\nu \rightarrow CO(a^3\Pi) + O(^3P)$	Model (K_1)	Lawrence (1972)
$CO_2 + e^-_{ph} \rightarrow CO(a^3\Pi) + O + e^-$	Model (K_2)	*Present work*
$CO + e^-_{ph} \rightarrow CO(a^3\Pi) + e^-$	Model	*Present work*
$CO_2^+ + e^- \rightarrow CO(a^3\Pi) + O$	K_3†	Seiersen et al. (2003); Rosati et al. (2003)
$CO(a^3\Pi) + CO_2 \rightarrow CO + CO_2$	1.0×10^{-11}	Skrzypkowski et al. (1998)
$CO(a^3\Pi) + CO \rightarrow CO + CO$	5.7×10^{-11}	Wysong (2000)
$CO(a^3\Pi) \longrightarrow CO + h\nu$	$K_4 = 1.26 \times 10^2$	Lawrence (1971)

e^-_{ph} = photoelectron.
†$K_3 = 6.5 \times 10^{-7}\ (300/Te)^{0.8} \times 0.87 \times 0.29\ cm^3\ s^{-1}$; here 0.87 is yield of dissociative recombination of CO_2^+ producing CO, and 0.29 is yield of $CO(a^3\Pi)$ produced from CO.
K_1, K_2, K_3, and K_4 are described in equation 3.

Table 2: Production rates (in $cm^{-3}\ s^{-1}$) with peak altitude for low solar activity condition (similar to Viking condition).

Production Process	Cameron band	CO_2^+ UV doublet
$CO_2 + h\nu$	465 at 137 km	391 at 131 km
$CO_2 + e^-_{ph}$	1470 at 128 km	95 at 127 km
$CO + e^-_{ph}$	81 at 130 km	-
$CO_2^+ + e^-$	267 at 133 km	-
Total	2094 at 131 km	478 at 131 km

e^-_{ph} = photoelectron.

Table 3: Overhead intensities (in kR) of CO Cameron and CO_2^+ UV doublet bands.

Emissions	EUVAC					SOLAR2000				
	hν+CO_2	e+CO_2	DR[§]	e+CO	Total	hν+CO_2	e+CO_2	DR	e+CO	Total
Low solar activity (Viking condition)										
Cameron band	1.2	3.7	0.6	0.2	5.8	1.8	5	1	0.3	8.2
UV doublet	1.1	0.2	-	-	1.3	1.4	0.3	-	-	1.7
SPICAM/Mars-Express, First Case (Ls $<$ 130°)										
Cameron band	1.4	5.4	1.6	0.4	8.8	2.1	5.7	1.8	0.4	10.1
UV doublet	1.4	0.4	-	-	1.8	1.6	0.4	-	-	2
SPICAM/Mars-Express, Second Case (Ls $>$ 130°)										
Cameron band	1.6	6.1	1.1	0.9	9.8	2.6	6.7	1.3	1	11.7
UV doublet	1.7	0.4	-	-	2.1	1.9	0.4	-	-	2.3
Higher solar activity (Mariner observations)										
Cameron band	2.3	11.8	2.4	1.7	18.3	3.6	10.2	2.2	1.6	17.7
UV doublet	3.1	0.8	-	-	3.9	2.8	0.7	-	-	3.5

[§]Dissociative recombination (e + CO_2^+).

Table 4: Overhead and limb intensities of different vibrational bands of CO Cameron band system calculated after reducing the e-CO_2 cross section by a factor of 2 in the first case (Ls $<$ 130°).

Band ($\nu' - \nu''$)	Band Origin Å	Overhead (R)		Limb (kR)[†]	
		EUVAC	S2K	EUVAC	S2K
0 - 0	2063.0	716	845	20	24
0 - 1	2158.4	713	840	20	23.2
0 - 2	2261.0	311	367	9	10
0 - 3	2374.0	79	93	2	2.6
1 - 0	1992.5	1151	1358	32	38
2 - 0	1927.5	603	711	17	20
3 - 0	1868.1	181	213	5	6
4 - 0	1813.0	38	45	1	1.3

[†]Limb intensities are given at altitude (120 km) of peak emission.

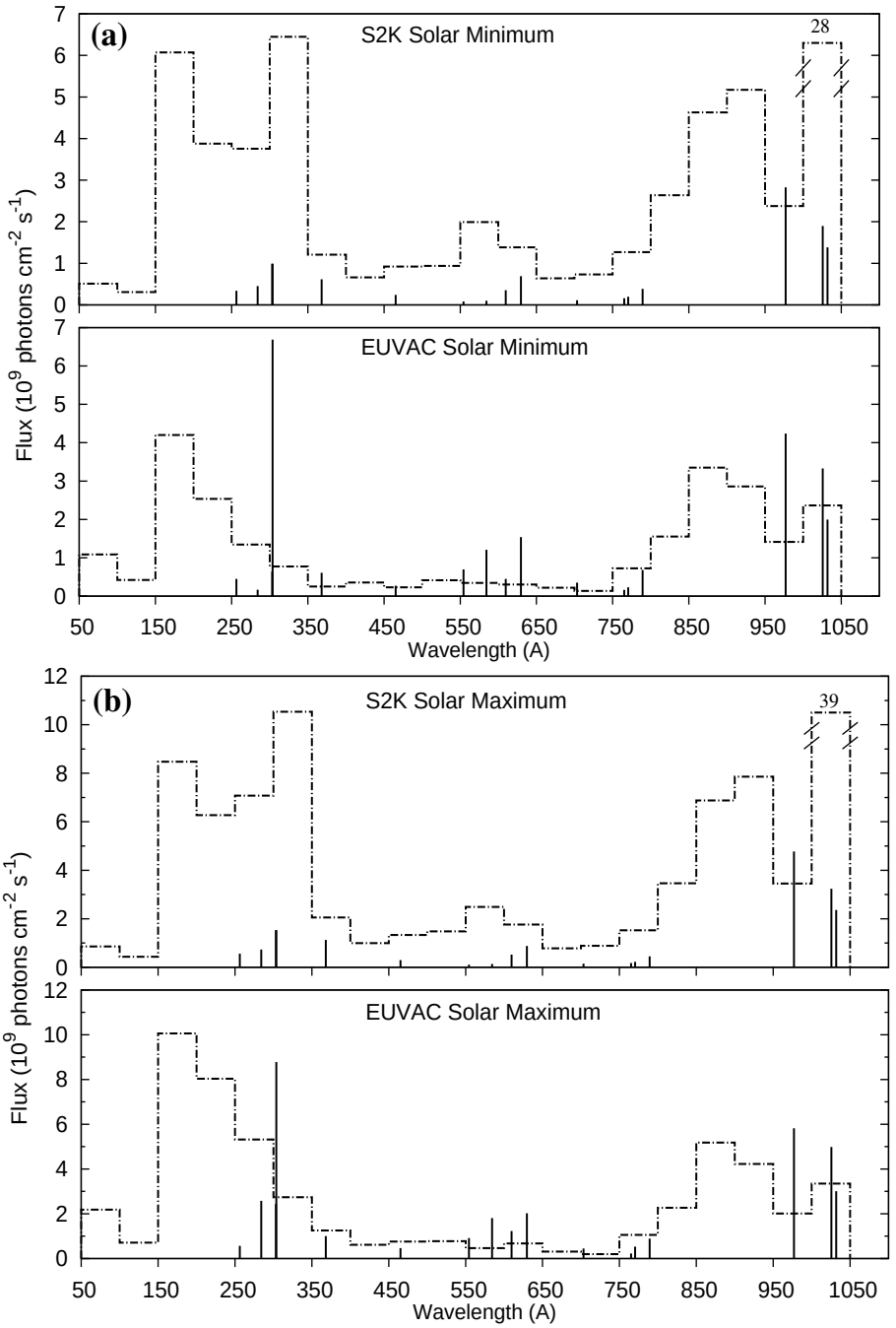

Figure 1: Solar photon flux, in bands and at lines, as a function of wavelength in EUVAC and S2K solar EUV flux models. (a) for the low solar activity condition on July 1976 (similar to Viking landing, F10.7 = 70), and (b) for high solar activity condition on August 1969 (similar to Mariner 6 and 7 observations period, F10.7 = 186).

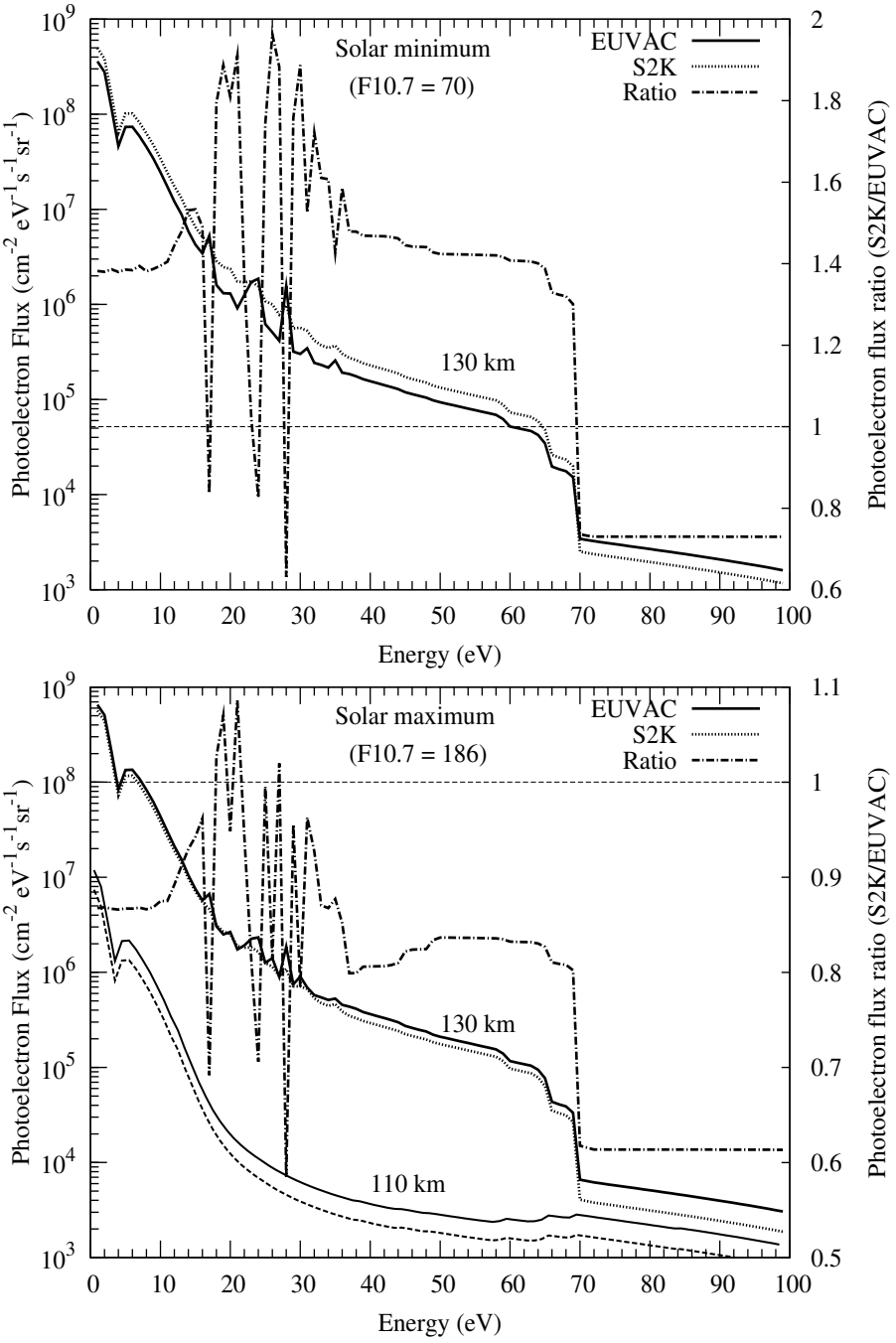

Figure 2: Calculated photoelectron fluxes for low (upper panel) and high (lower panel) solar activity conditions at SZA = 45°. The ratio of the photoelectron flux at 130 km calculated using the two solar flux models is also shown with magnitude on right side Y-axis. Thin dotted horizontal line depicts the S2K/EUVAC ratio = 1.

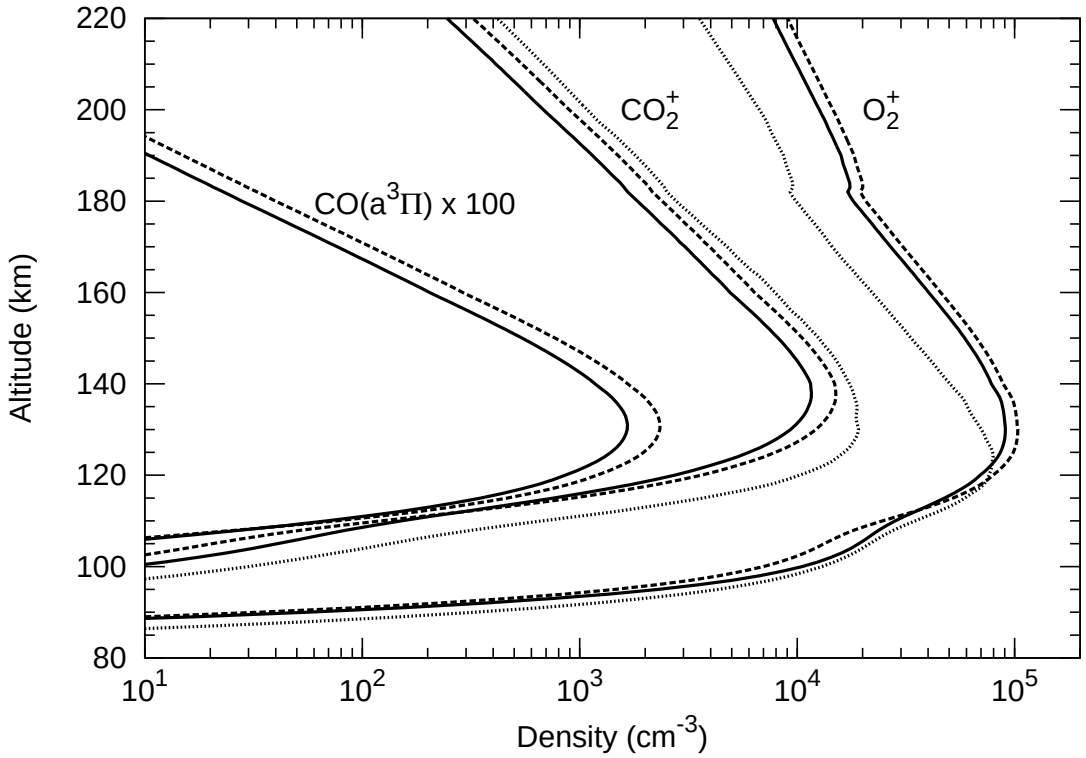

Figure 3: Densities of CO_2^+ and O_2^+ ions and $CO(a^3\Pi)$ molecule for solar minimum condition calculated using EUVAC (solid curve) and S2K (dashed curve) solar EUV flux models. Density of $CO(a^3\Pi)$ molecule is plotted after multiplying by a factor of 100. Dotted curves show the densities of CO_2^+ and O_2^+ ions for first case (Ls $< 130°$) using EUVAC solar flux.

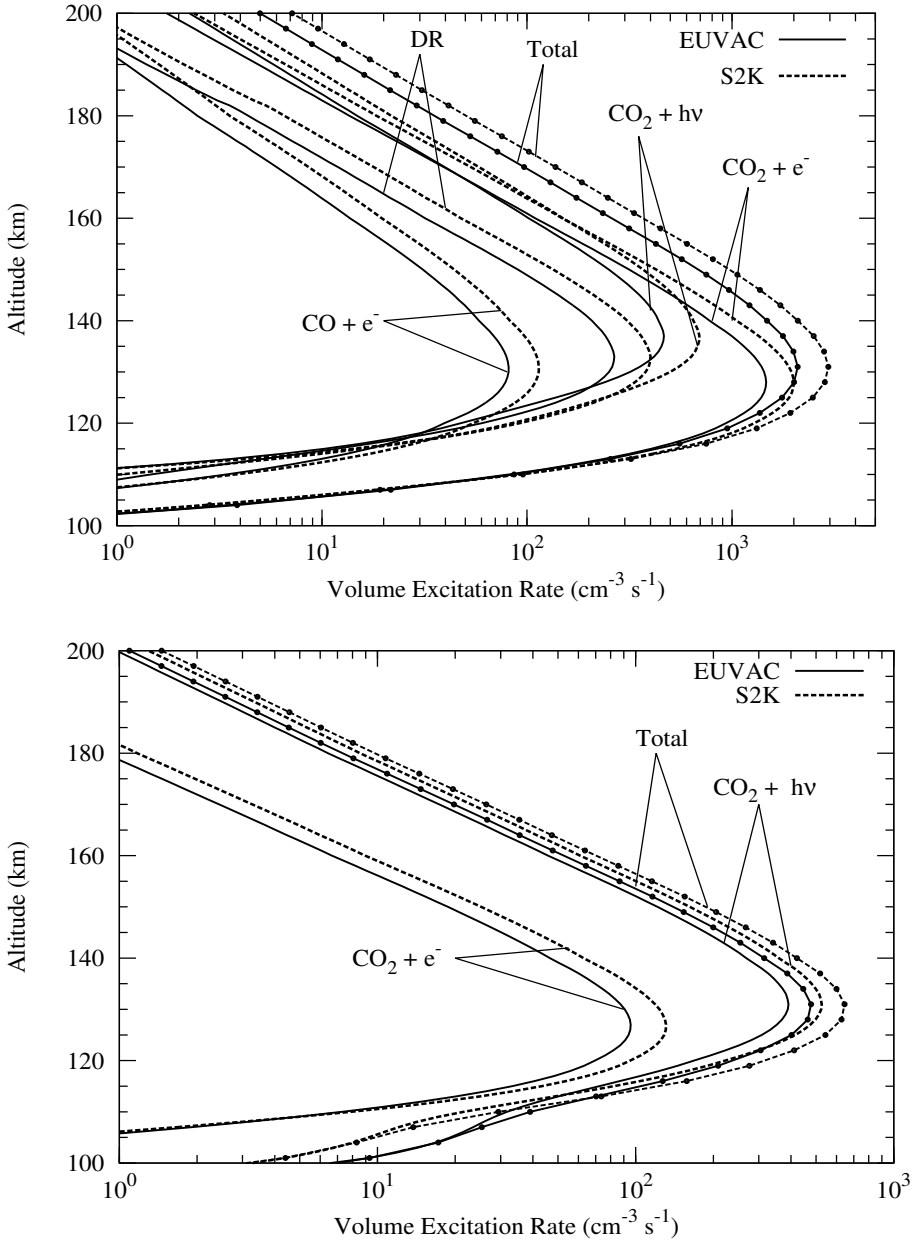

Figure 4: Calculated production rates of the CO($a^3\Pi$) (upper panel) and $CO_2^+(B^2\Sigma_u^+)$ (bottom panel) for low solar activity condition (Ls∼100–140°). DR stands for dissociative recombination.

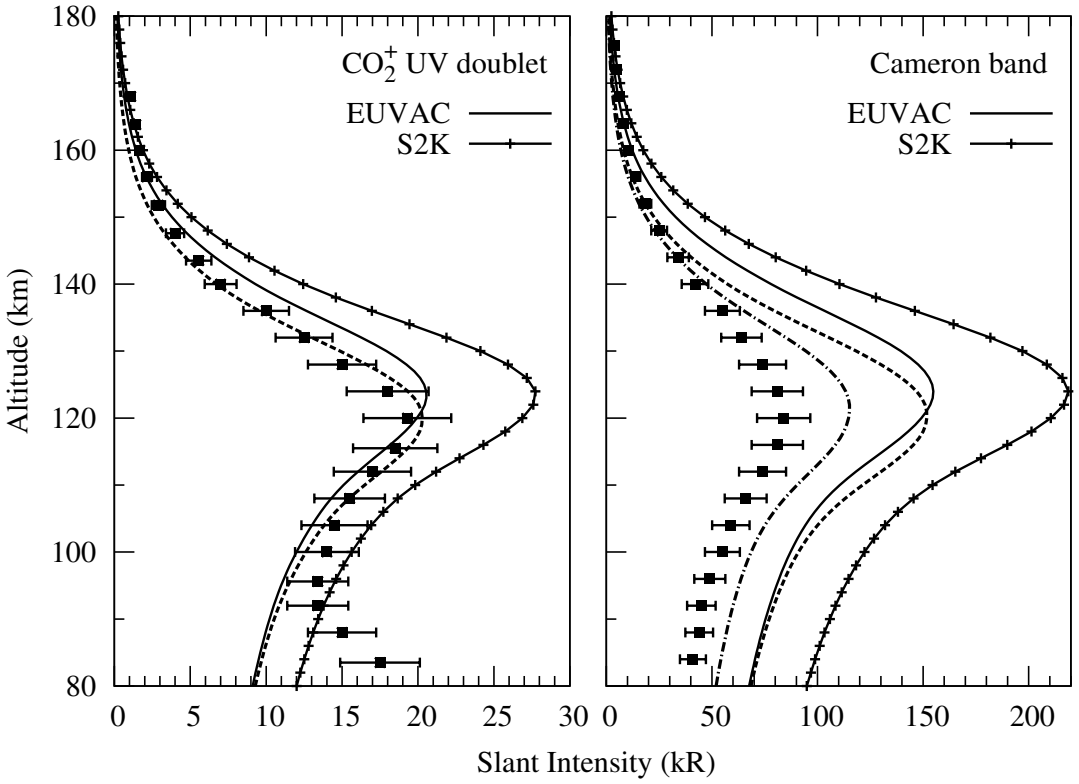

Figure 5: Calculated limb profiles of CO_2^+ UV doublet bands (left panel) and CO Cameron (right panel) for low solar activity condition. Solid squares with error bars represents the SPICAM-observed values taken from Simon et al. (2009). Dashed curves show the calculated intensity (using EUVAC model) after reducing the density of CO_2 by a factor of 1.5. Dash-dotted curve shows the calculated intensity (using EUVAC) of Cameron band with reduced density (by a factor of 1.5) and reduced (by a factor of 2) e-CO_2 Cameron band production cross section.

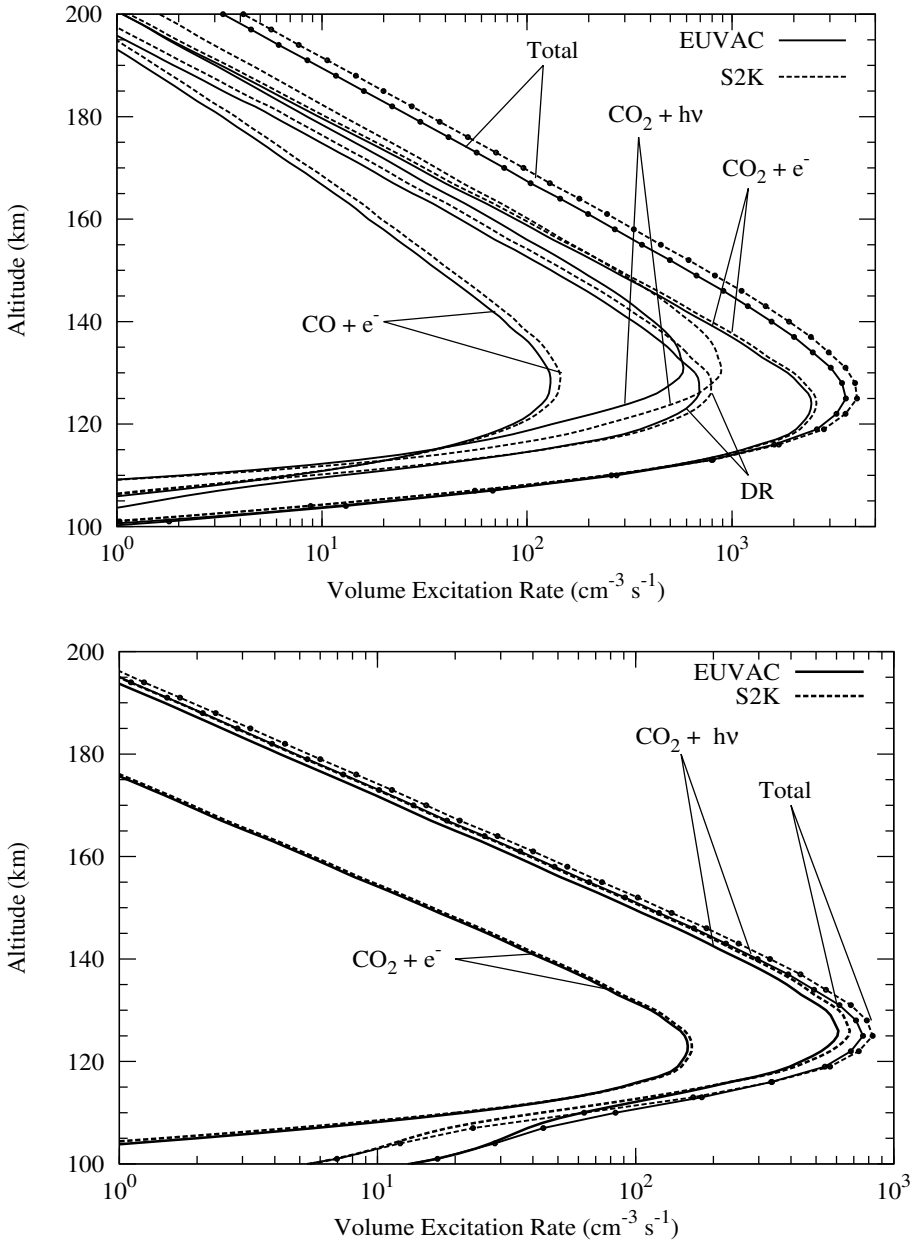

Figure 6: Calculated production rates of the CO($a^3\Pi$) (upper panel) and $CO_2^+(B^2\Sigma_u^+)$ (bottom panel) for solar longitude Ls $< 130°$. DR stands for dissociative recombination.

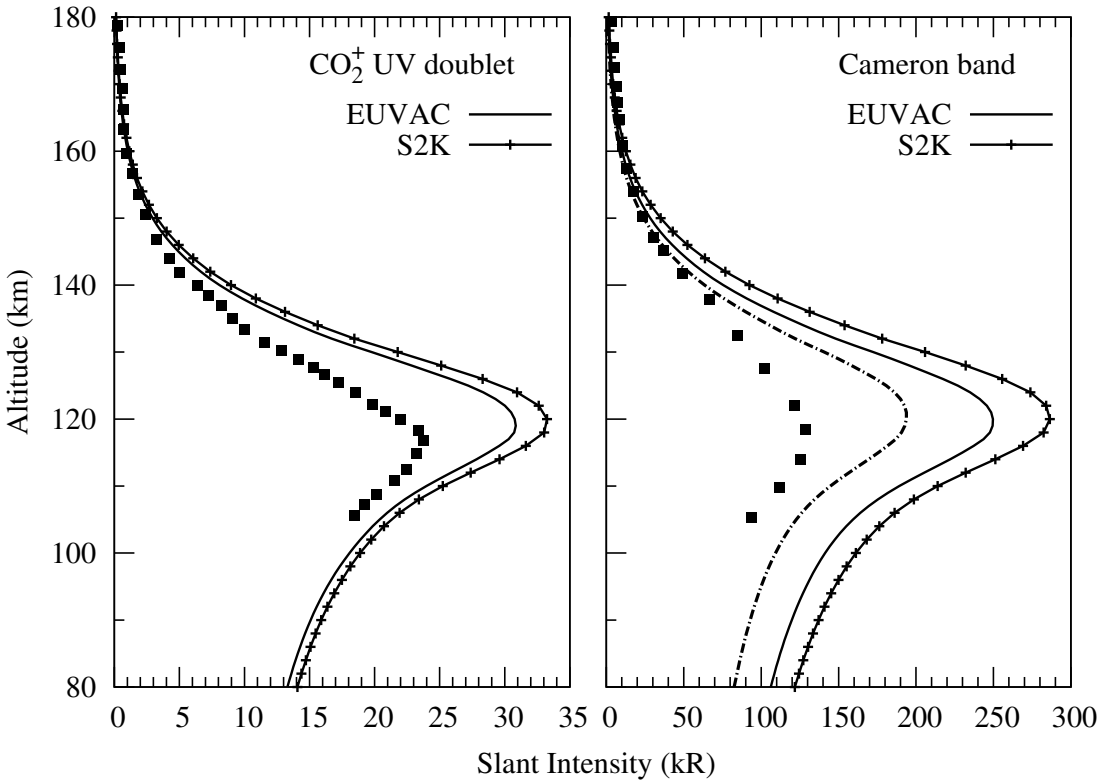

Figure 7: Calculated limb profile of CO_2^+ UV doublet band (left panel) and CO Cameron band (right panel) for Ls $<$ 130°. Symbols represent the SPICAM-observed values taken from Leblanc et al. (2006). Dash-dotted curve shows the calculated intensity of Cameron band with reduced (by a factor of 2) e-CO_2 cross section.

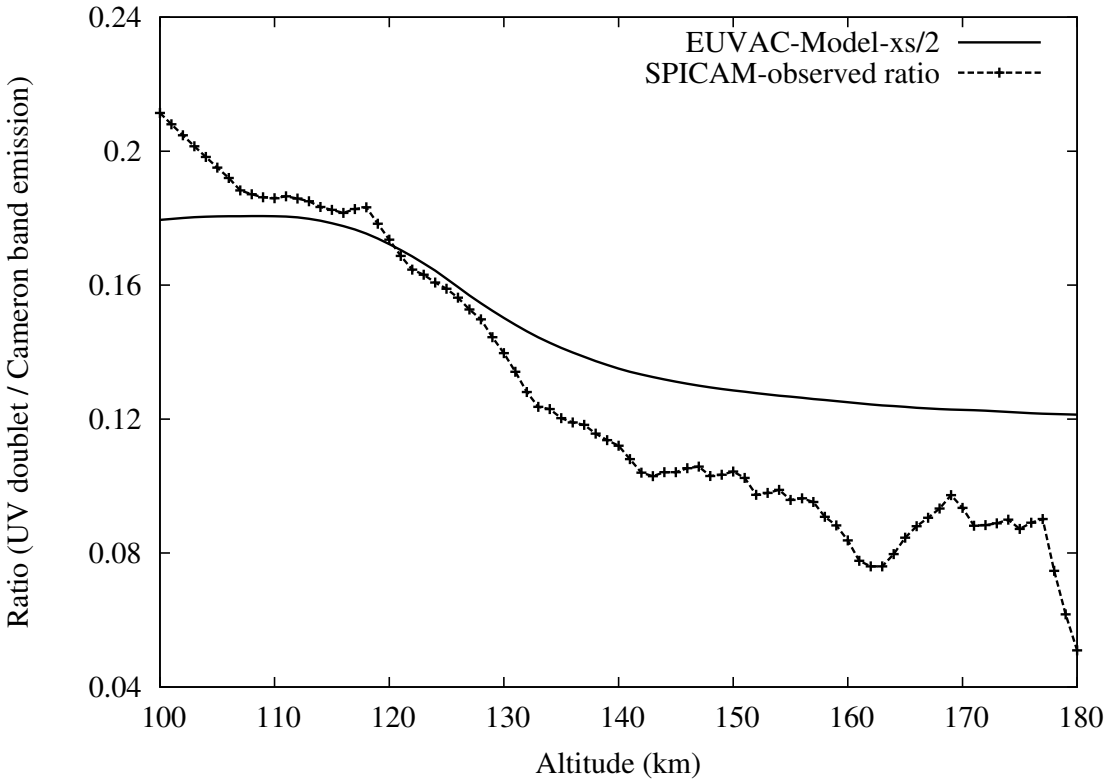

Figure 8: Altitude variation of intensity ratio of UV doublet and CO Cameron band system. Calculated ratio is shown for EUVAC solar flux model with Cameron band production cross section in e-CO_2 collision is reduced by a factor of 2. SPICAM-observed ratio is from Fig. 9(a) of Leblanc et al. (2006).

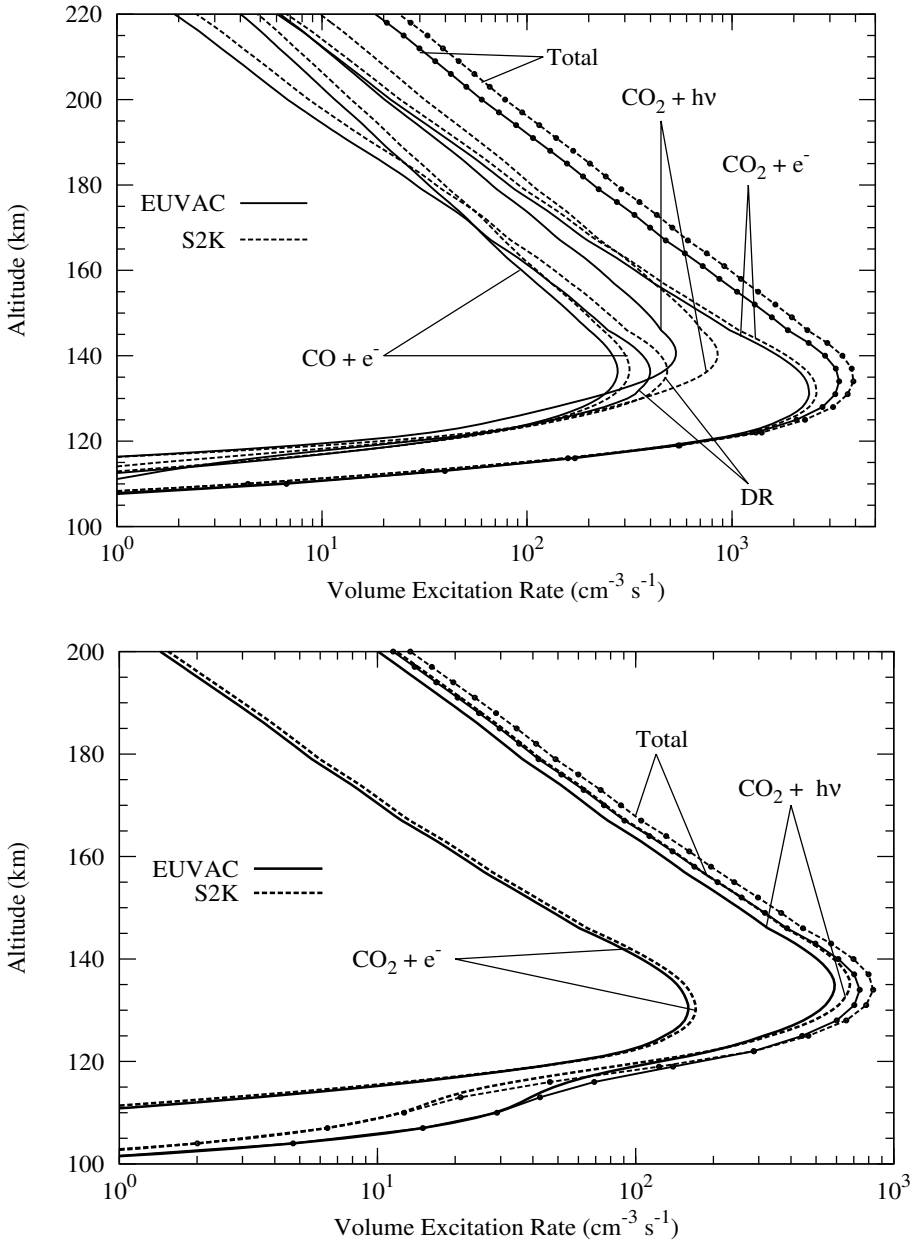

Figure 9: Calculated production rates of the CO($a^3\Pi$) (upper panel) and $CO_2^+(B^2\Sigma_u^+)$ (bottom panel) for solar longitude Ls $> 130°$. DR stands for dissociative recombination.

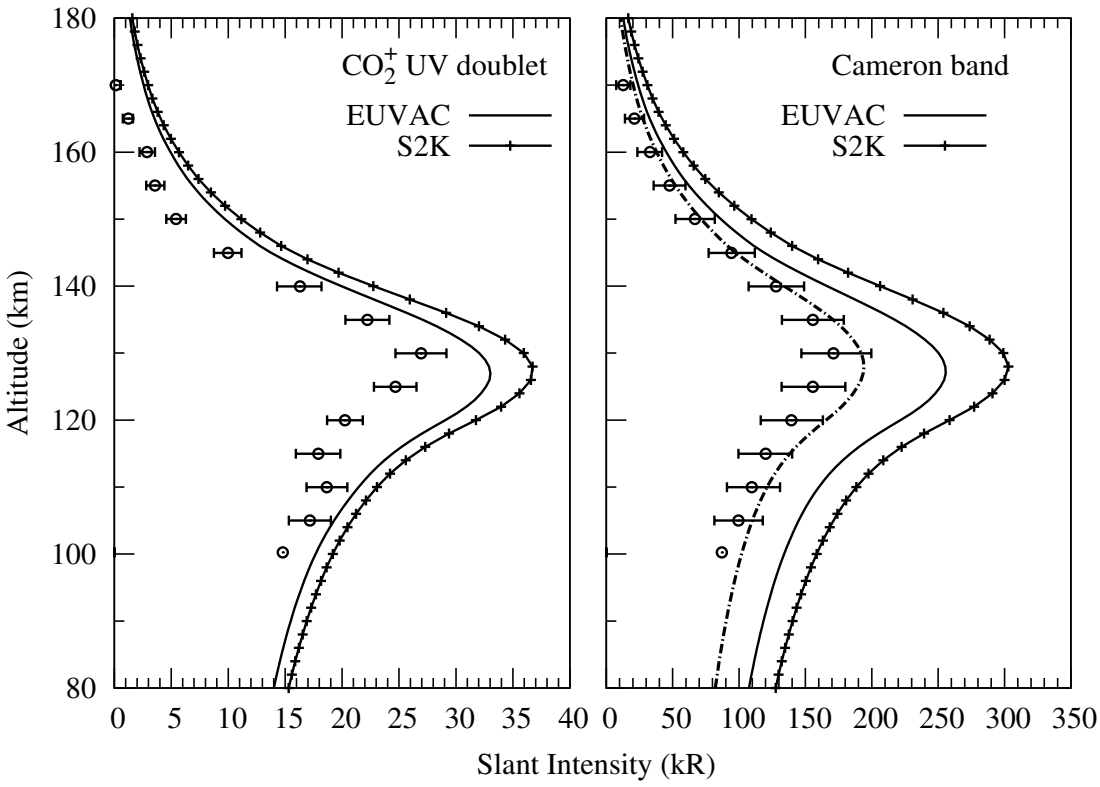

Figure 10: Calculated limb profiles of CO_2^+ UV doublet band (left panel) and CO Cameron band (right panel) for Ls $> 130°$. Dash dotted curve shows the Cameron band intensity for EUVAC model with e-CO_2 cross section forming CO($a^3\Pi$) reduced by a factor of 2. Open circles with error bars represent the SPICAM-observed intensity taken from Shematovich et al. (2008).

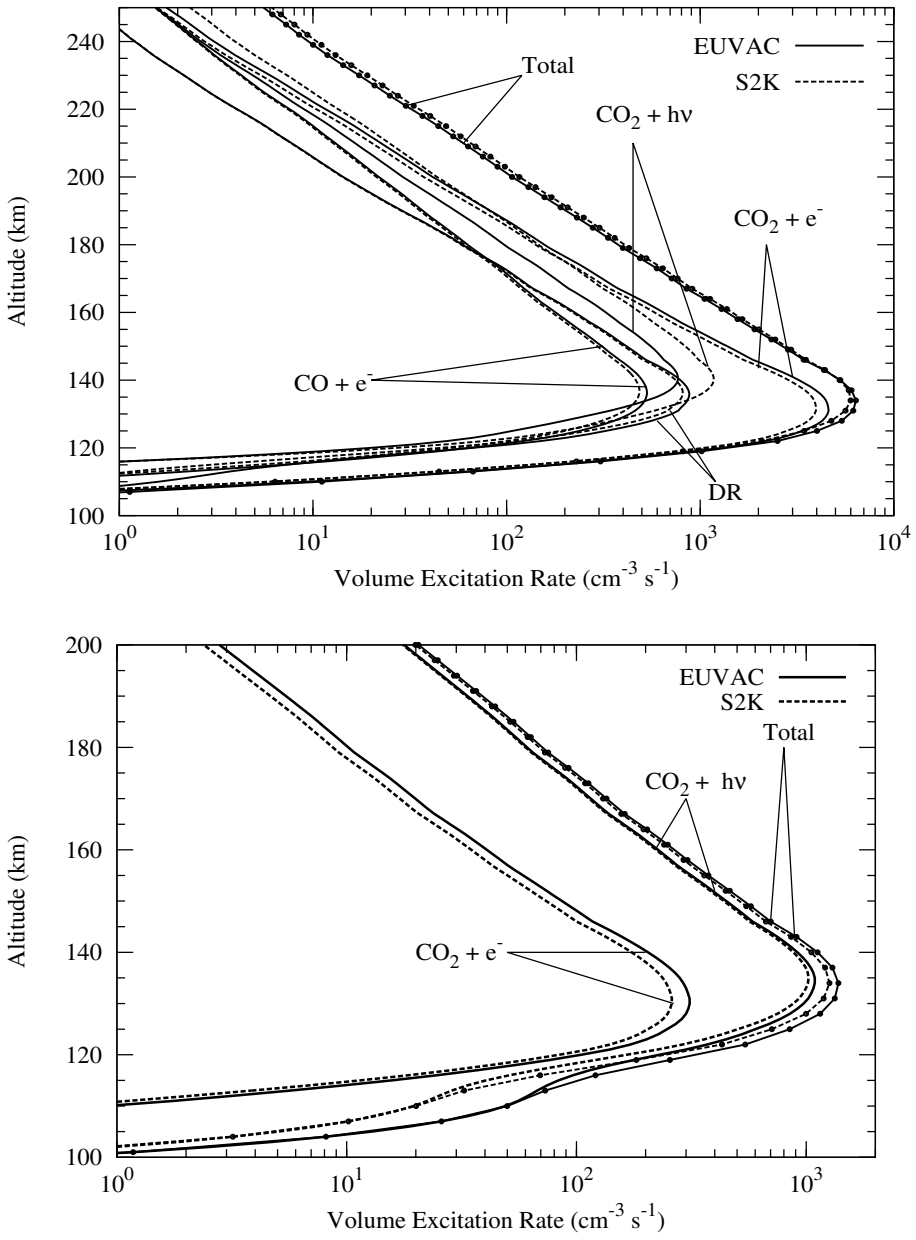

Figure 11: Calculated production rates of the $CO(a^3\Pi)$ (upper panel) and $CO_2^+(B^2\Sigma_u^+)$ (bottom panel) for solar maximum condition. DR stands for dissociative recombination.

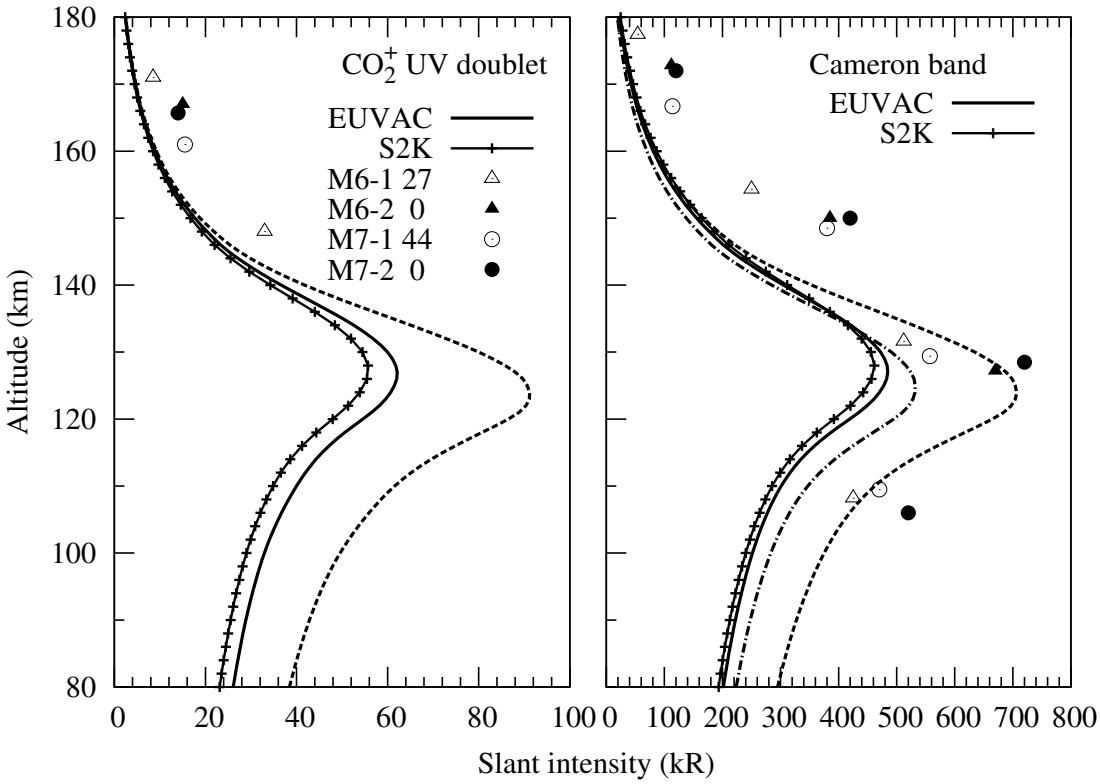

Figure 12: Calculated limb intensity for the higher solar activity condition similar to Mariner 6 and 7 flybys. Solid curve shows the intensity calculated using EUVAC model at SZA = 45°. Solid curve with symbols shows the limb intensity calculated using S2K model at SZA = 45°. Dashed curve shows the calculated intensity (using EUVAC model) at SZA = 0°. Dash dotted curve shows the calculated intensity (using EUVAC model) at SZA = 0° and after reducing the e-CO_2 cross sections forming CO($a^3\Pi$) by a factor of 2. Symbol represents the observed intensity of Cameron band and UV doublet band measured by Mariner 6 and 7 (Stewart, 1972). Observed values are shown for 2 orbits each of Mariner 6 (for SZA = 27 and 0°; open and solid triangle, respectively) and Mariner 7 (for SZA = 44 and 0°; open and solid circle, respectively).